Aust. J. Phys., 1984, **37**, 321–57

A New Look at Radio Supernova Remnants

B. Y. Mills, A. J. Turtle, A. G. Little and J. M. Durdin

School of Physics, University of Sydney, Sydney, N.S.W. 2006.

Abstract

Catalogues are presented of radio supernova remnants in both Large (LMC) and Small (SMC) Magellanic Clouds together with maps of the LMC remnants prepared at a frequency of 843 MHz and with a resolution of 43×45 arcsec. The 38 confirmed remnants are believed to represent a reasonably complete sample for diameters less than about 40 pc although the LMC catalogue is probably very incomplete for larger diameters. The supernova remnants (SNRs) are compared with the Galactic remnants in the catalogue of Clark and Caswell (1976) and they are found to be similar in many ways. In particular a distance scale derived from the Cloud SNRs reproduces well the mean distances of directly measured Galactic calibrators. The usual model of a SNR expanding adiabatically from a small diameter is not supported by the statistics of the number–diameter relation which suggest that rapid expansion up to quite large diameters is common. The physical implications are discussed. A supernova rate of about four per century is derived for the Galaxy and about one per century for the two Magellanic Clouds combined.

1. Introduction

The physical properties and evolution derived for SNRs depend critically on distance scales and their freedom from systematic bias. However, determination of the distances, either of individual remnants or of statistical samples, has always been a major problem. The difficulties of obtaining a reliable unbiassed selection of Galactic calibrators is well known and it is evident that one way to overcome this problem is to study remnants in external galaxies but, until recently, selection effects imposed by sensitivity and resolution have rendered this approach relatively ineffective. Much work has been done on the Magellanic Clouds and, because of their proximity, these are clearly the most effective galaxies to study.

The commissioning of the Molonglo Observatory Synthesis Telescope (MOST) in 1981 and the Einstein Observatory has now provided the essential instrumental advances necessary to obtain statistically valid results on the radio SNRs in these galaxies. At the distances of the Magellanic Clouds, the sensitivity of the MOST appears sufficient to avoid selection effects, but the resolution is not quite adequate to resolve a few with very small diameters. To study the latter adequately, higher resolution will be needed in the future.

The present results are based on a series of observations using the MOST, carried out in late 1981 and 1982. They involved checking the radio emission of all likely SNR candidates selected from the Einstein Observatory X-ray surveys (Long *et al.*

0004-9506/84/030321$02.00

1981; Seward and Mitchell 1981) together with candidates from earlier radio and optical work. An overall survey was also made of the SMC. The X-ray surveys are found to be very efficient for detecting remnants of small to intermediate diameters and it is believed that the sample presented here is reasonably complete for diameters up to about 40 pc. Many larger remnants will undoubtedly be discovered as the result of completing the LMC survey but the present sample is certainly more complete than any other sample of remnants currently available.

2. Observations

The MOST is a unique rotational synthesis telescope in which a map is synthesized in real time from a comb of fan beams which can be arranged to track a point in the sky for 12 h. The principal features have been described by Mills (1981) and Durdin *et al.* (1984); it operates at a frequency of 843 MHz. Observations used in the present work began shortly after commissioning the telescope in mid 1981 and were completed in December 1982. During this time the telescope underwent many changes and developments, principally an improvement in general stability and an expansion of the synthesized field from about 11 to 46 arcmin. The r.m.s. noise was measured as between 0·3 and 0·4 mJy (1 Jy $\equiv 10^{-26}$ W m^{-2} Hz^{-1}) for a full synthesis and correspondingly higher when mapping a larger field in the multiplexing mode. The beamwidth is 43×43 cosec δ arcsec, the first sidelobe is -8% and more distant sidelobes are less than 1% in magnitude. 'Cleaning' of the maps has been carried out only when necessary to clarify structural features of the radio sources; the principal effect is to remove the large negative sidelobe.

The first set of observations on the SMC, in September–October 1981, has been described by Mills *et al.* (1982). They mainly involved full synthesis of 11 arcmin fields, although some observations utilized a mode in which several fields were sampled sequentially. The X-ray catalogue of Seward and Mitchell (1981) was used to select 16 SNR candidates; four of these were confirmed as remnants, together with two earlier radio–optical identifications. Following these observations, a similar program was carried out on the LMC during October–December 1981. The X-ray catalogue of Long *et al.* (1981) was used to select candidates which were observed together with various previously suggested remnants from radio or optical observations. A preliminary account of these observations has been given by Mills (1983); altogether 23 remnants were confirmed in the LMC with six listed as possible remnants, requiring further work for confirmation.

During September–December 1982, some additional observations were made. These included a survey of the major part of the SMC in which 13 overlapping 46 arcmin maps were made (Mills and Turtle 1984). These maps were searched for apparently shell-like structures or generally extended sources not obviously due to thermal emission from the bright emission nebulae catalogued by Henize (1956) and Davies *et al.* (1976). Particular attention was given to regions near the X-ray sources listed by Inoue *et al.* (1983).

All the previous six SNRs stood out prominently and, in addition, six more possible remnants were recognized; two of these were shell sources with apparently non-thermal spectra and four others were extended sources which were too weak to have been observed by other instruments. Three of the latter had apparent shell-like structures and the fourth coincided with a faint catalogued nebulosity; all four were

close to X-ray sources catalogued by Inoue *et al.* (1983). These six new possible SNR identifications were studied optically by Mt Stromlo astronomers, using the Anglo–Australian telescope, in a cooperative program which resulted in the confirmation of five (Mathewson *et al.* 1984) bringing the total SNR content of the SMC to 11. The sixth object was too faint in both radio and optical emission to come to any conclusion. In the optical program, one of the previously listed 'possible' SNRs in the LMC was also confirmed.

No additional SNR candidates were observed in the 1982 LMC program, but observations were made to improve the accuracy and quality of some of the previous maps and some additional areas were mapped. The new observations, together with additional X-ray observations (Mathewson *et al.* 1983), provided confirmation of three more of the six possible SNRs originally listed in the LMC; the total of confirmed remnants is now 27. Two remain classified as 'possible' SNRs requiring further observations.

3. Properties of the SNRs

The measured radio properties of the confirmed and 'possible' SNRs are listed in Tables 1–3. In each table the columns contain the following information:

Column 1: The IAU designation of the radio source.

Column 2: The estimated right ascension of the radio centroid.

Column 3: The estimated declination of the radio centroid (rounded to 10 arcsec for large sources).

Column 4: S, the integrated flux density in mJy of the remnant at 843 MHz, separated as far as possible from any neighbouring H II regions. The standard error for well observed SNRs is about 10% but increases for low brightness or confused objects. When the error is likely to exceed ~20% a colon follows.

Column 5: L, the absolute luminosity of the remnant in units of 10^{16} W Hz^{-1} at 843 MHz on the assumptions that the LMC is at a distance of 55 kpc and the SMC at 63 kpc.

Column 6: θ, the angular diameter of the remnant in arcmin. Because the small diameter remnants are not completely resolved by the radiotelescope and complex structure sometimes adds to the uncertainty of all sizes, a standard procedure has been adopted to define an 'equivalent diameter'. Two models, comprising a thin circular ring and a uniform circular disc have been fitted to the half-power responses along the major and minor axes. The diameter quoted is the mean of these four results and is expected to give a reasonable approximation to the actual size for SNRs of typical morphology. When the process appears to lead to an uncertain result a colon follows. To avoid statistical bias, the same procedure has been carried out even when the SNR is well resolved.

Column 7: D, the spatial diameter measured in pc using the distance assumptions above.

Column 8: D_o, the spatial diameter of the optical remnants given by Mathewson *et al.* (1983, 1984).

Table 1. Supernova remnants in the LMC

(1) Radio source	(2) Position (1950) R.A. h m s	(3) Dec. ° ′ ″	(4) S (mJy)	(5) L ($10^{16}\times$ W Hz^{-1})	(6) θ (min)	(7) D (pc)	(8) D_0 (pc)	(9) Σ ($10^{-20}\times$ W m^{-2} Hz^{-1} sr^{-1})	(10) α	(11) Notes
0453–685	04 53 47	−68 34 11	211	7·6	1·2	20	36	2·03	−0·38	LHG1, A1
0454–665	04 54 43	−66 30 17	170	6·1	1·0	16	15	2·56	−0·42	N11L, DEM34a, A2
0455–687	04 55 53	−68 43 40	380	13·7	3·2	51	53	0·56	−0·38	LHG2, N86, DEM33, A3
0500–702	05 00 20	−70 12 20	66:	2·4:	1·9	30	31	0·28		LHG7, N186D, A4
0505–679	05 05 49	−67 56 48	9·6	0·35	0·55	9	20	0·46		LHG10, DEM71, A5
0506–680	05 06 02	−68 05 45	430	15·5	0·75	12	11	11·50	−0·69	LHG11, N23, A6
0509–687	05 09 12	−68 47 14	753	27·1	<0·4	<7	6	>59		LHG13, N103B, DEM84
0509–675	05 09 35	−67 34 54	82	3·0	<0·4	<7	7	>6·4	−0·48	LHG14
0519–697	05 19 08	−69 42 10	488	17·6	1·5	24	28	3·26		LHG23, N120, A7, Note[A]
0519–690	05 19 52	−69 05 03	145	5·2	<0·4	<7	8	>11·3	−0·65	LHG26
0520–694	05 20 07	−69 28 52	141	5·1	2·3	37	32	0·40	−0·48	LHG27, A8
0525–660	05 25 18	−66 01 40	845	30·5	1·9	30	29	3·61	−0·68	LHG34, A9
0525–696	05 25 25	−69 41 10	6980	252	1·4	22	29	55·5	−0·59	LHG35, N132D, A10
0525–661	05 25 55	−66 07 30	2066	74·5	1·0	16	17	31·1	−0·45	LHG36, N49, DEM190, A11
0527–658	05 27 51	−65 52 20	166:	6·0:	3·8	61	56	0·17	−0·45:	LHG39, DEM204, A12
0528–692	05 28 03	−69 14 30	172:	6·2	1·9	30	38	0·74		LHG40, SMC2, Note[B]
0532–710	05 32 35	−71 02 20	591	21·3	2·7	43	47	1·23	−0·40	LHG47, N206, A13
0534–699	05 34 28	−69 57 00	137	4·9	2·1	33	30	0·48	−0·59	LHG53, A14
0534–705	05 34 47	−70 35 20	129	4·7	2·3	37	46	0·36	−0·59	LHG54, DEM238, A15
0535–660	05 35 40	−66 03 49	2106	75·9	0·75	12	6	56·3	−0·56	LHG59, N63A, DEM243, A16, Note[C]

0536–706	05 36 42	−70 40 20	85	3·1	1·9	30	39	0·36	−0·52	LHG61, DEM249, A17
0538–691	05 38 06	−69 11 49	1700:	61·3:	0·8:	13:	7	38·7:		LHG67, N157B, A18, Note[D]
0538–693	05 38 35	−69 23 10	214	7·7	2·5	40	43	0·51		SMC2, Note[E]
0540–693	05 40 32	−69 21 19	1055	38·0	0·55	9	2	50·1	−0·43	LHG79, A19, Note[F]
0543–689			100:	3·6:	2·8:	45:	76	0·19:	−0·29:	LHG82, DEM299, A20, Note[G]
0547–697	05 47 34	−69 43 10	1300	47·0	3·1	50	56	2·00	−0·49	LHG88, N135, DEM316, A21
0548–704	05 48 24	−70 25 40	97	3·5	1·4	22	28	0·77		LHG89, A22

[A] The strong unresolved source to the north is probably a background object. The arc-like structure corresponds to the emission nebula N120 and has a thermal spectrum except at the position of the SNR, but confusion effects prevent a reliable determination of the index for the SNR.

[B] The tabulated flux density includes the coincident small diameter source of flux density about 50 mJy. However, this may be a background object so the flux density is indicated to be uncertain.

[C] The elongated source to the north–west is apparently a background object. The X-ray remnant has a diameter of 19 pc (Mathewson *et al.* 1983) so that there is an unusual diversity of sizes.

[D] The SNR is superimposed on an H II region from which it is difficult to separate with the present resolution. The angular size and flux density are therefore both uncertain although the combined spectrum is very flat (Mills *et al.* 1978). Both the X-ray and optical sizes given by Mathewson *et al.* (1983) are substantially smaller than our estimate of the radio size.

[E] This SNR appears to have a non-thermal spectrum from the data of Clarke *et al.* (1976) but an estimate of the index is not possible because of confusion. It has no X-ray counterpart.

[F] The radio structure appears complex and extended which is inconsistent with the optical and X-ray data (Mathewson *et al.* 1983). Some of the radio emission could be originating in a very close background source. There is also radio emission from the nebulosity in the west, extending southwards (N158A).

[G] A badly defined remnant. It is very faint and there is a background confusion problem because of the proximity of the very bright 30 Doradus region.

Table 2. Supernova remnants in the SMC

(1) Radio source	(2) Position (1950) R.A. h m s	(3) Dec. ° ′ ″	(4) S (mJy)	(5) L ($10^{16}\times$ W Hz^{-1})	(6) θ (min)	(7) D (pc)	(8) D_0 (pc)	(9) Σ ($10^{-20}\times$ W m^{-2} Hz^{-1} sr^{-1})	(10) α	(11) Notes
0045–734	00 45 26	−73 24 40	300:	12·2	1·5:	27:	26	1·72:		T2, SMC1
0046–735	00 46 34	−73 35 50	133	6·3	1·8	33	31	0·60		T4, SMC1
0047–735	00 47 17	−73 30 50	35	1·7	2·0	36	51	0·15		T5, SMC2
0049–736	00 49 24	−73 37 40	122	5·8	2·2	40	29	0·37	−0·4	IE 0049·4–7339, T6, SMC1/2
0050–728	00 50 57	−72 53 30	116	5·5	2·8	50	58	0·23		N50, DEM68, SMC2. Note[A]
0056–725	00 56 37	−72 33 34	79	3·75	2·3	42	56	0·22		T16, SMC2
0058–718	00 58 42	−71 49 30	160	7·6	2·7	48	62	0·34		SMC2, Note[B]
0101–724	01 01 38	−72 26 03	107	5·1	1·3	23	25	0·99		IE 0101·5–7226, T21, SMC1
0102–722	01 02 24	−72 17 57	384	18·2	0·45	8	7	29·3		IE 0102·2–7219, T22, SMC1
0103–726	01 03 34	−72 39 20	103	4·9	3·0	54	57	0·17	−0·5	IE 0103·3–7240, T23, SMC1
0104–723	01 04 45	−72 21 30	13	0·62	1·3	23	29	0·12		T25, DEM131, SMC2, Note[C]

[A] No X-ray counterpart has been detected but the relevant 408 MHz map of Clarke *et al.* (1976) shows emission at the position of the remnant which indicates a non-thermal spectrum. However, confusion prevents an estimate of the index. The radio brightness is higher than one might expect from its classification as 'bright' in the Hα catalogue of Davies *et al.* (1976).

[B] From the data of Clarke *et al.* (1976) the radio source has clearly a rather steep non-thermal spectrum but confusion prevents estimation of the index. No X-ray counterpart has been detected.

[C] The radio brightness is little more than might be expected from its classification as a 'bright' H II region by Davies *et al.* (1976) and it is too faint for spectral measurements. However, there is an associated X-ray source and no identifiable exciting stars for the nebulosity. Mathewson *et al.* (1984) commented on the sharpness of the optical filaments and the similarity of the spectrum to the Balmer dominated SNRs in the LMC, which include the SNR 0505–679 of even lower luminosity. Although some doubt must exist it is reasonable to classify it as an SNR.

Table 3. Possible supernova remnants in the Magellanic Clouds

(1) Radio source	(2) Position (1950) R.A. h m s	(3) Dec. ° ′ ″	(4) S (mJy)	(5) L ($10^{16}\times$ W Hz^{-1})	(6) θ (min)	(7) D (pc)	(8) D_0 (pc)	(9) Σ ($10^{-20}\times$ W m^{-2} Hz^{-1} sr^{-1})	(10) α	(11) Notes
0536–692	05 36 32	−69 13 50	1045	37·7	5·9	95		0·57		A23, Note[A]
0543–678	05 43 28	−67 52 00	256	9·2	6·5	100	120	0·12	−0·0:	N70, DEM301, A24, Note[B]

[A] This ring source was listed by Clarke *et al.* (1976) as two sources corresponding to the western and eastern concentrations (0536–692B and 0537–692A). They concluded that the western source has a thermal spectrum and the eastern possibly a non-thermal spectrum. A direct comparison with our integrated flux density is not possible because of confusion and zero level uncertainties. An X-ray source is catalogued close to the eastern boundary (LHG62).

[B] N70 has long been regarded as a possible SNR but it is clear from our results that the spectrum is quite flat and the non-thermal spectrum deduced by Milne *et al.* (1980) was the result of resolution problems. Nevertheless, for the reasons advanced in Section 6 we continue to regard it as a possible old SNR.

Column 9: Σ, the mean surface brightness of the remnant at 843 MHz in units of $10^{-20}\,\mathrm{W\,m^{-2}\,Hz^{-1}\,sr^{-1}}$.

Column 10: α, the radio spectral index ($s \propto \nu^{\alpha}$) is given only if relatively unconfused measurements are available at different frequencies, particularly 408 MHz (Clarke *et al.* 1976) or 5 GHz (McGee *et al.* 1972; Milne *et al.* 1980). Flux densities at 5 GHz inferred from the data of Mathewson *et al.* (1983) have also been used.

Column 11: References are given to catalogued X-ray or optical counterparts as follows: LHG (Long *et al.* 1981); IE (Seward and Mitchell 1981); T (Inoue *et al.* 1983); N (Henize 1956); DEM (Davies *et al.* 1976). Map references are made to the Appendix of this paper, denoted A, the paper by Mills *et al.* (1982), denoted SMC1, or the paper by Mathewson *et al.* (1984) denoted SMC2. The Appendix includes 24 LMC maps in which the map can provide information additional to that in the tables. All the SMC remnants have been mapped in the two references cited.

4. Statistics of the Cloud SNRs

The process of selection of candidates and confirmation of the Cloud SNRs should have resulted in an essentially complete sample of small and intermediate sized remnants. The primary X-ray data from which we selected most of our candidates are very efficient for detecting these. However, there is a rapid reduction of apparent X-ray luminosity with increasing size (Long 1983) which must result in a significant proportion of large diameter remnants falling below the X-ray detection threshold. For example, the survey of the SMC by Seward and Mitchell (1981) recorded emission from only four of our eleven catalogued remnants. The deeper survey by Inoue *et al.* (1983), even when pushed to a detection limit of 3σ, recorded nine remnants, but two large remnants were undetected although they were quite strong radio emitters. For the LMC, where only one of the confirmed SNRs was not included as an X-ray source in the survey by Long *et al.* (1981), it might be expected that more large diameter remnants will be found when the remainder of the Cloud is surveyed with the MOST. In the following analysis a diameter of 40 pc has been adopted as the upper limit for those statistics which involve an assumption of completeness.

(*a*) *Comparisons between the Clouds*

In order to obtain the best statistical estimates of SNR properties it is desirable to combine the data for both Clouds. However, it is first necessary to establish that there are no gross differences between them. The selection against large diameter remnants in the LMC is evident in the following tabulation:

	Number of SNRs		
	$D \leqslant 10$ pc	$10 < D < 40$ pc	$D \geqslant 40$ pc
LMC	5	16	6
SMC	1	5	5

On the basis of these numbers, one might expect about ten more large diameter remnants to be found in the LMC eventually, but no other discrepancies are evident.

A more sensitive test is to compare the geometric mean luminosities and diameters for SNRs with diameters less than 40 pc, the assumed complete sample:

	LMC	SMC
$\langle \log L \rangle$	$16{\cdot}98 \pm 0{\cdot}13$	$16{\cdot}66 \pm 0{\cdot}22$
$\langle \log D \rangle$	$1{\cdot}24 \pm 0{\cdot}06$	$1{\cdot}36 \pm 0{\cdot}10$

These results suggest a relative preponderance of high luminosity and small diameter remnants in the LMC. However, the differences are not significant at the 5% level so that, bearing in mind the possibility of a real difference, it is reasonable for statistical purposes to combine the data from both Clouds to obtain a representative sample of extragalactic remnants.

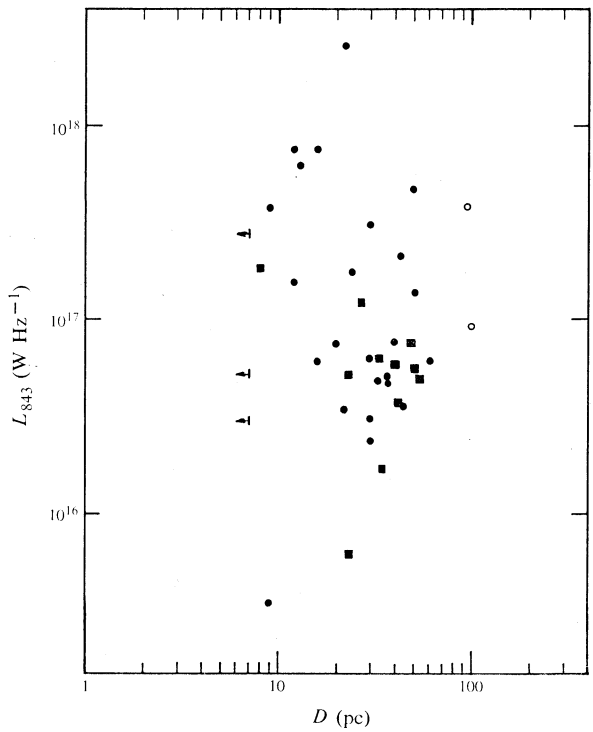

Fig. 1. Distribution of radio luminosity for SNRs in both Clouds as a function of their radio diameter. Solid circles and solid squares represent the identified SNRs in the LMC and SMC respectively. Open circles are the 'possible' SNRs in the LMC. Upper limits are shown for the diameters of three SNRs in the LMC.

(*b*) *Luminosity–Diameter Relation*

It is customary to discuss the emission of SNRs as a function of size using the brightness–diameter (Σ–D) relation. This is a useful statistic in appropriate applications because only one of the quantities is distance-dependent, but it can sometimes be misleading because of the strong dependence of Σ on D ($\Sigma \propto 1/\theta^2$). For the Clouds, at a known distance, it is more natural to use the independent absolute luminosity in place of the mean brightness when looking for a possible relation between radio emission and size.

In Fig. 1 all the data for both Clouds are assembled in an L–D diagram which summarizes the results of our observations. The large scatter is most striking; another obvious and significant result is the sharp cutoff for $L \lesssim 3 \times 10^{16}$ W Hz^{-1}, well above the sensitivity limit of the radiotelescope. The sharp cutoff and the associated asymmetry in the distribution of luminosities are illustrated by the histogram in Fig. 2.

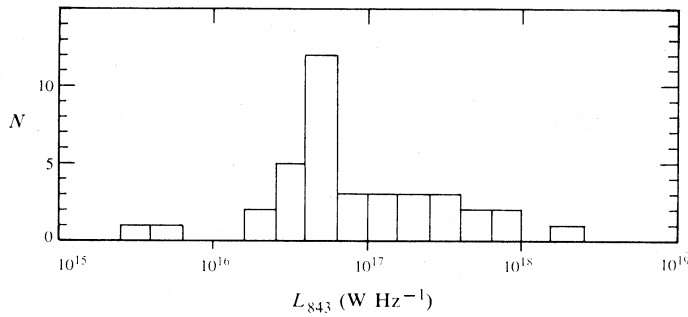

Fig. 2. Histogram for radio luminosities of the identified SNRs in both Clouds.

The regression of $\log L$ on $\log D$ yields a correlation coefficient of $-0{\cdot}1$, which has no significance, as expected from the appearance of the scatter diagram. Formally we also obtain (with errors)

$$\log L = -0{\cdot}29 \log D + 17{\cdot}34$$
$$\pm 0{\cdot}33 \qquad \pm 0{\cdot}09.$$

In order to investigate the effects of observational selection we may calculate two more regressions in which:

(i) The two very weak radio emitters 0104–723 and 0505–679 are omitted. This gives a correlation coefficient of $-0{\cdot}3$ at an apparent significance level of 10% and

$$\log L = -0{\cdot}52 \log D + 17{\cdot}73$$
$$\pm 0{\cdot}28 \qquad \pm 0{\cdot}08.$$

(ii) The three SNRs of small angular size which could not be resolved are also omitted. These deletions lead to a correlation coefficient of $-0{\cdot}5$ at an apparent significance level of less than 1% and

$$\log L = -1{\cdot}00 \log D + 18{\cdot}45$$
$$\pm 0{\cdot}34 \qquad \pm 0{\cdot}08.$$

These results demonstrate the strong effects of selection on the derived properties of SNRs. However, they also suggest that a significant relation might be discernible for the larger remnants and this is also suggested by inspection of the scatter diagram. If we restrict attention to diameters $D \geqslant 10$ pc, the correlation coefficient is $-0{\cdot}4$ at a significance level of 2% and

$$\log L = -1{\cdot}10 \log D + 18{\cdot}62$$
$$\pm 0{\cdot}43 \qquad \pm 0{\cdot}08.$$

This result suggests a relation for intermediate and large remnants of the form $L \propto D^{-1\pm0\cdot4}$. This is, in fact, the relation obtained in earlier work with strongly selected remnants.

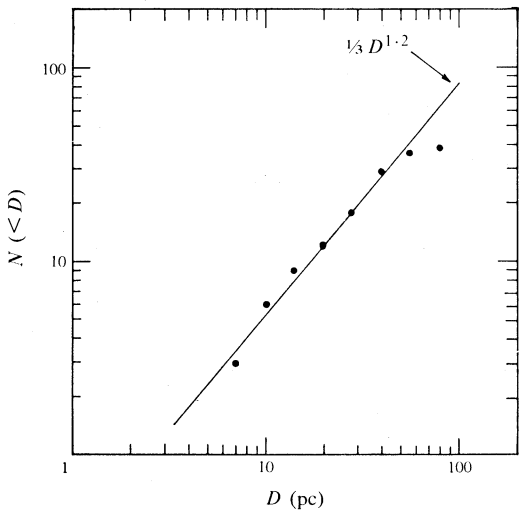

Fig. 3. Number–diameter relation for the identified SNRs in both Clouds. The solid line represents the maximum likelihood slope for SNRs with diameters between 7 and 40 pc.

(*c*) *Number–Diameter Relation*

The *N–D* relation for all catalogued SNRs is shown in Fig. 3. It is well known from work on radio source counts that the derivation of meaningful results from integral counts is not straightforward. Here we use the maximum likelihood method (Crawford *et al.* 1970) which is readily adapted for the angular size statistic and is known to provide unbiassed estimates and a realistic error. Assuming the relation to be of the form $N \propto D^{\beta}$, where N is the number of remnants with diameters less than D pc, we have carried out the analysis for a range of sizes from 7 to 40 pc. The three unresolved SNRs with unknown diameters less than 7 pc are therefore not used. There are 24 SNRs in this sample and we find $\beta = 1\cdot2\pm0\cdot36$. The statistical uncertainty has been increased by limitation of the range, but this cannot be avoided if an objective measure is to be obtained. A solid line of this slope is shown in Fig. 3; it has the equation

$$N = \tfrac{1}{3}D^{1\cdot2}.$$

5. Comparison of Cloud and Galactic SNRs

The *N–D* relation for the Clouds is different from the corresponding relation which has been accepted for Galactic SNRs (see e.g. Clark and Caswell 1976); these remnants were considered to be in the 'Sedov' expansion phase for which $N \propto D^{2\cdot5}$. It is therefore important to establish whether there is a basic difference between the remnants in the Clouds and the Galaxy or whether the apparently different slopes for the *N–D* relation have arisen because of errors or selection effects. The only distance-independent check which can be made is based on the surface brightness statistic.

(*a*) *Number–Brightness Relations for Clouds and Galaxy*

This is a simple test for similarity between the two populations but incompleteness causes uncertainties. Both populations are incomplete for large-diameter low-brightness remnants. In addition the Galactic population could also be incomplete for small-diameter relatively high-brightness remnants which are likely to have been discarded as extragalactic objects.

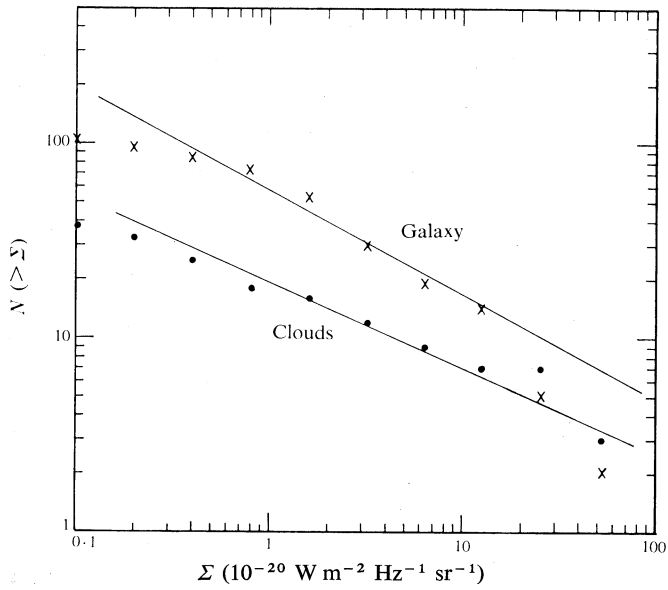

Fig. 4. Number–brightness relations for the Clouds (circles) and the Galaxy (crosses). The lines represent the maximum likelihood slopes for $\Sigma \geqslant 5\times10^{-21}$ W m^{-2} Hz^{-1} sr^{-1}.

In Fig. 4 we compare the present results on the Clouds with a distribution obtained from the catalogues of Clark and Caswell (1976) at 408 MHz. Their tabulated brightnesses are multiplied by 0·72 to allow for a mean spectral index of −0·45. To estimate the slope of these distributions we confine attention to brightnesses greater than 5×10^{-21} W m^{-2} Hz^{-1} sr^{-1}. This is the mean brightness corresponding to a linear diameter of 40 pc for SNRs in the Clouds, as found from the relation determined in Section 5*d*. If we assume that the relations are of the form $N(>\Sigma) \propto \Sigma^{\gamma}$, the results are as follows:

	Number of remnants	γ
Clouds	23	$-0\cdot44\pm0\cdot09$
Galaxy	82	$-0\cdot53\pm0\cdot06$

In Fig. 4 we show lines defined by

$$N = 3\cdot0\times10^{-8}\Sigma^{-0\cdot44} \quad \text{and} \quad N = 1\cdot5\times10^{-9}\Sigma^{-0\cdot53}$$

for the Clouds and Galaxy respectively. Within the statistical uncertainties there is no difference between the derived slopes. Incompleteness in both catalogues introduces additional uncertainties but there is clearly no evidence here that the SNR populations of the Clouds and Galaxy differ.

(*b*) *Radio Distance Scale for SNRs*

To compare Galactic and Cloud SNRs further it is necessary to derive a distance scale based on measurements of flux density and angular size. This is derived for the homogeneous sample of remnants at known distances in the Clouds and compared with various Galactic distance calibrators. Because of the very large scatter in luminosities, the scale cannot be very accurate for individual remnants but is suitable for some statistical comparisons.

Mills (1983) used a simple luminosity scale based on the mean luminosity of the Cloud SNRs. However, this may be refined and made more accurate for individual remnants by making use of the distance independent brightness Σ to improve the estimate of luminosity. A 'diameter' scale may also be used in which the diameter of a remnant is estimated from a measurement of Σ. It may be shown that these apparently different physical approaches are mathematically identical.

To derive a scale suitable for application to the Galaxy the two very low luminosity remnants, 0104–723 and 0505–679, have been rejected; similar remnants are not included among the Galactic calibrators. The three unresolved remnants have been included using their optical diameters in the belief that this will give a more realistic relation. For the regressions of $\log L$ and $\log D$ on $\log \Sigma$ we obtain

$$\begin{aligned} \log L &= \quad 0{\cdot}45 \log \Sigma + 25{\cdot}85 \\ &\quad\ \pm 0{\cdot}06 \qquad\ \pm 0{\cdot}05, \\ \log D &= -0{\cdot}275 \log \Sigma - 4{\cdot}05 \\ &\quad\ \pm 0{\cdot}03 \qquad\ \pm 0{\cdot}03. \end{aligned}$$

These lead to the distance scale

$$d = 46 S_{843}^{-0.275} \theta^{-0{\cdot}45},$$

where d is the distance in kpc, S_{843} is the flux density in Jy at 843 MHz and θ is the angular diameter in minutes of arc.

To apply this scale to the catalogue of Clark and Caswell (1976) at 408 MHz we assume a mean spectral index of $\alpha = -0{\cdot}45$ and obtain

$$d = 50 S_{408}^{-0.275} \theta^{-0{\cdot}45}.$$

If it is assumed that L and D are uncorrelated, an equivalent scale may be derived by calculating two distances, one based on the mean luminosity of the Cloud SNRs and the other based on their mean diameter, and taking the geometric mean. Applying this method we find the very similar result

$$d = 53 S_{843}^{-\frac{1}{2}} \theta^{-\frac{1}{2}}.$$

The earlier equation will be adopted as it was derived using a formally correct procedure.

The errors to be expected for individual distances may be estimated by applying the scale to determine the distance of the Cloud SNRs in our sample. Taking the geometric means of the individually derived distances, the results are as follows:

	LMC	SMC
$\langle d \rangle$	53 kpc	65 kpc
s.e.	8%	7%
σ	41%	26%

The mean distances for the LMC and SMC are well reproduced as would be expected. The accuracy in individual distances is substantially worse in the LMC, presumably because of the wider range of diameters and flux densities represented. By considering the results for both Clouds, a dispersion of between 30% and 40% might be expected from use of the distance scale for Galactic SNRs.

(*c*) *Galactic Distance Calibrators*

Clark and Caswell (1976) listed two types of Galactic calibrators: (i) those based on optical observations to estimate the distance either directly from association with objects at a known distance or from expansion velocities and (ii) those based on radio absorption line measurements of various types which yield kinematic distances relative to an assumed distance to the Galactic centre.

We define a distance ratio R which is the ratio of the distance determined by our distance scale to that given by Clark and Caswell:

(i) For nine optical calibrators (excluding SNR 1006 which has a different distance criterion and an anomalous result) we find

$$R = 1{\cdot}08 \pm 0{\cdot}08, \qquad \sigma = 24\%.$$

(ii) Considering the 13 kinematic calibrators given highest weight by Clark and Caswell we find

$$R = 0{\cdot}78 \pm 0{\cdot}10, \qquad \sigma = 37\%.$$

(iii) If all 31 kinematic calibrators are included, some of which give only lower limits to the distance, we find

$$R \leqslant 0{\cdot}96 \pm 0{\cdot}09, \qquad \sigma = 50\%.$$

These results are satisfactory, particularly since the kinematic distances are based on a distance to the Galactic centre of 10 kpc. Current evidence points to a smaller distance; a distance of 7·8 kpc, which would make the ratio R equal to unity, is quite acceptable. It is interesting to base all distances on the optical calibrators. These would then give distances to the Magellanic Clouds of 49 and 60 kpc, and a distance to the Galactic centre of 7·2 kpc. Both these results and the earlier comparison support the view that there are no substantial differences between the radio properties of the Galactic and Cloud remnants.

(*d*) *Galactic Number–Diameter Relation*

The N–D relation cannot be observed directly in the Galaxy as there is no independent method of determining the distances of the great majority of remnants. In principle it may be obtained from the N–Σ relation but the result depends critically on the relation assumed between Σ and D. As an example of the difficulty, Clark and Caswell (1976) derived a slope of $\beta = 2{\cdot}5$ based on Galactic calibrators, whereas Mills (1983), using the same catalogue but applying a simple 'luminosity' distance scale based on the Cloud observations, derived a slope of $\beta = 1{\cdot}15$.

Direct application of our present distance scale to individual remnants is inappropriate for determining the N–D relation as the scale is effectively based on the regression of $\log D$ on $\log \Sigma$ and will therefore give a statistically biassed estimate. An unbiassed estimate may be obtained by using the regression of $\log \Sigma$ on $\log D$ to convert the

N–Σ relation to an N–D relation. Thus, if we define $N(>\Sigma) = g\Sigma^{\gamma}$ and $\Sigma = dD^{\delta}$, we obtain

$$N(>D) = gd^{\gamma} D^{\gamma\delta}.$$

To obtain the regression of $\log\Sigma$ on $\log D$, all our Cloud SNRs must be used; even the faintest can appear in the Galactic catalogue. We obtain

$$\log\Sigma_{843} = -2{\cdot}30\log D - 16{\cdot}63$$
$$\pm 0{\cdot}33 \qquad \pm 0{\cdot}09.$$

Using the N–Σ relations derived in Section 5*a* we have for $D \leqslant 40$ pc

$$\text{Galaxy} \quad N = 1{\cdot}0D^{1{\cdot}2\pm 0{\cdot}34},$$
$$\text{Clouds} \quad N = 0{\cdot}6D^{1{\cdot}0\pm 0{\cdot}34}.$$

We may have some confidence that the process gives a realistic estimate for the Galaxy as it has reproduced well the directly observed slope for the Clouds. It has, of course, been assumed that the Σ–D relation for the Galaxy is the same as that for the Clouds. This assumption is consistent with all the evidence that we have presented but it may be directly tested by using the Galactic calibrators listed by Clark and Caswell (1976). If we confine attention to the 22 calibrators for which actual distances have been given rather than lower limits, a regression analysis for Σ on D gives a slope of $-2{\cdot}8\pm 0{\cdot}4$, not inconsistent with our slope of $-2{\cdot}3\pm 0{\cdot}3$. If the SNRs Cas A and the Crab nebula are rejected as being atypical because of their exceptionally high brightnesses, the slope for the remainder is reduced to $-2{\cdot}4\pm 0{\cdot}4$ in even better agreement with the Cloud results. However, even these calibrators are overluminous when compared with the general Cloud population so that the agreement may be fortuitous. A steep slope for the Galactic N–D relation can be obtained by including Cas A among the calibrators and by restricting the N–Σ analysis to relatively high brightnesses (corresponding to smaller diameters) where the slope is steeper, possibly due to the incompleteness already discussed. Incompleteness at both large and small diameters is probably the major cause of uncertainties in the Galactic N–D relation; the quoted statistical errors are probably lower limits.

(*e*) *Supernovae Birthrates in Galaxy and Clouds*

Making the assumption that populations in the Clouds and Galaxy are statistically identical we may use the historical supernovae to calibrate the evolutionary time scale, following the method of Clark and Caswell (1976). Analysis of the N–Σ relation in Section 5*a* indicates that the ratio between the numbers of remnants catalogued in the Galaxy and in the Clouds is about 3·5 : 1. Adopting the N–D relation for the Clouds as derived in Section 4*c* and assuming a ratio of the populations of 4 : 1 to allow for a slightly greater incompleteness in the Galaxy than in the Clouds, we may write for the Galactic number–diameter relation, $N = 1{\cdot}3D^{1{\cdot}2}$. Assuming that all supernovae have produced detectable remnants and that no 'deaths' occur within times equal to the maximum historical ages, we have

$$1{\cdot}3D^{1{\cdot}2} = N = t/\tau,$$

where τ is the mean time between supernova outbursts and t is the mean time for a remnant to reach diameter D. Thus, making the further assumption that historical remnants are typical, we can derive an estimate of τ from each such remnant:

$$\tau = t/1{\cdot}3D^{1{\cdot}2}.$$

Results from eight historical remnants discussed by Clark and Stephenson (1977*a*) are shown in Table 4. The diameter D_1 is obtained from the distance scale of Section 5*b* and the diameter D_2 from the measured distance quoted by Clark and Caswell (1976).

Table 4. Historical supernovae and derived birthrates

Super-nova	Radio source	t (yr)	D_1 (pc)	D_2 (pc)	τ_1 (yr)	τ_2 (yr)
AD 185	G 315·4−2·3	1800	32	28	22	25
386	G 11·2−0·3	1600	12	⩾6·1	62	⩽140
393	G 348·5+0·1	1590	13(13)	23·8(15·1)	57(57)	28(47)
	(or G 348·7+0·3)					
1006	G 327·6+14·5	980	39	12·8	9·3	36
1054	G 184·6−5·8	930	5·1	3·0	102	192
1181	G 130·7+3·1	800	13	⩾12·1	29	⩽31
1572	G 120·1+1·4	410	13	⩾13·8	15	⩽14
1604	G 4·5+6·8	380	11	9·3	16	20

According to Clark and Stephenson the supernova of AD 393 may be identified either with G 348·5+0·1 or G 348·7+0·3. We list both results but for definiteness accept the first. The geometric means of all these results are

$$\langle\tau_1\rangle = 29\pm8\ \text{yr}, \qquad \langle\tau_2\rangle \leqslant 39\pm11\ \text{yr}.$$

Three of the calibrators should perhaps be rejected: AD 1054 (the Crab nebula) because it is an atypical remnant, AD 1006 because the distances are quite inconsistent, and AD 386 for which the identification is given as uncertain. The corresponding means are

$$\langle\tau_1\rangle = 24\pm5\ \text{yr}, \qquad \langle\tau_2\rangle \leqslant 23\pm5\ \text{yr}.$$

It appears that the best estimate for τ is close to 25 yr which, in view of the uncertainties, is better expressed as an occurrence rate of four per century. For the Clouds, with about one quarter the number of remnants, the corresponding rate is about one per century. The Galactic rate is close to that obtained by Srinivasan and Divarakanath (1982) using a very different approach. It is also compatible with rates derived from supernovae observed in external galaxies (Tammann 1977) and from an analysis of optical selection effects on the historical supernovae (Clark and Stephenson 1977*b*).

If we assume a slope of 1·7 for the N–D relation, which is the maximum which can reasonably be accommodated by the statistics, we find that the Galactic rate is reduced to about three per century but the scatter in individual estimates is very much increased.

By adopting our best estimate, two other statistics may be derived:

(i) the age of a remnant $t \approx 33D^{1{\cdot}2}$;

(ii) the mean velocity of expansion

$$\langle V\rangle = D/2t \approx D^{-0{\cdot}2}/60\ \text{pc yr}^{-1}$$
$$\approx 15000D^{-0{\cdot}2}\ \text{km s}^{-1}.$$

It should be noted that these results do not necessarily represent the evolution of some typical remnant but the ensemble averages for remnants of the same diameter. They can be applied only when the diameter is more than a few pc.

Finally we note that for $D = 10$ pc the mean age is about 500 yr. Thus we might expect about 20 young remnants in the Galaxy with diameters less than 10 pc. Among the calibrators of Clark and Caswell there are 11 listed with diameters possibly less than 10 pc. Probably not all the young remnants will have yet developed radio emission but it is likely that a number remain to be discovered, as discussed earlier. One possible small diameter remnant has been suggested in the direction of the Galactic centre (Goss *et al.* 1983). Applying our distance scale to the measured flux density and angular size we find a distance of 7·6 kpc, a diameter of 7 pc and an age of $\sim$300 yr. However, our scales are unreliable at the extremes of size so that the evidence that the radio source is actually located close to the nucleus depends entirely on the positional coincidence.

6. SNR Evolution

Perhaps the most significant result of this work is the small slope found for the N–D relation. It has been generally believed that SNRs spend the greater part of their lifetime expanding adiabatically in the 'Sedov' phase which predicts a relation of the form $N \propto D^{2.5}$. As a result of direct measurement it is evident that the majority of Cloud remnants does not follow such a relation, as indeed has been suggested by Clarke (1976), and the evidence we have presented indicates that most of the Galactic remnants do not follow it either. A new assessment of the normal evolution of an SNR seems to be required.

Numerous analyses of supernova evolution have been carried out using tractable models of uniform spherical shells of ejecta expanding into a uniform interstellar gas of average density. This leads to the rapid establishment of the adiabatic phase which then persists for tens of thousands of years. An assumption can be made that the interstellar medium is clumpy with most of the volume occupied by tenuous gas which delays the onset of adiabatic expansion and results in a long period spent in more rapid expansion with, roughly, $N \propto D^{1.7}$ (McKee and Ostriker 1977). However, when sufficient material has been accumulated by the expanding shell it eventually reverts to the adiabatic phase. An analysis of a model in which an irregular shell of ejecta expands in a clumpy medium has not been attempted but it might be expected that the N–D relation would show a still smaller slope and the onset of the adiabatic phase would be further delayed. Whatever the process, it is inevitable that the remnant is eventually slowed to normal cloud velocities, probably passing through the adiabatic phase and then into the 'momentum-conserving' phase for which the relation $N \propto D^4$ is even steeper. As a steep N–D relation is not observed at any diameter, a straightforward conclusion is that non-thermal radio emission does not persist for very long after slowing has become significant.

Little attention has been given to the early life of a remnant before it enters the adiabatic phase but an approximate description may be derived very simply. We may reasonably assume that the ejecta energy is initially dominated by the kinetic energy of expansion (a temperature of $\sim 10^{10}$ K would be needed for equality of thermal and kinetic energies). As the interstellar material is swept up, the kinetic energy is thermalized, heating the swept up material and thereby producing an internal

pressure which aids the expansion. The development of full adiabatic expansion occurs when the kinetic energy has been reduced to 28% of the total (for a monatomic gas) and it remains constant at this proportion thereafter (Chevalier 1974).

The earliest stages are therefore controlled by simple momentum conservation and, if we make the simplifying assumption that the velocity of the swept up material is equal to the velocity of the ejecta at any time, we have the relations

$$V = V_0(1+M_s/M_e)^{-1}, \qquad \mathrm{KE} = E_0(1+M_s/M_e)^{-1},$$

where V is the velocity of expansion, KE is the kinetic energy, V_0 and E_0 are the initial velocity and energy respectively, M_s is the swept up mass and M_e the mass of the ejecta. In general these equations will give lower limits to the expansion velocity and kinetic energy. If, however, we adopt them as describing approximately the early stages of the expansion we see that, at $M_s = M_e$, half the kinetic energy will have been converted to thermal energy and at $M_s = 3M_e$ three-quarters will have been converted; the adiabatic regime will then be close to establishment. For this regime, with $\mathrm{KE} = 0{\cdot}28E_0$, we obtain

$$V = 0{\cdot}53V_0(1+M_s/M_e)^{-\frac{1}{2}}.$$

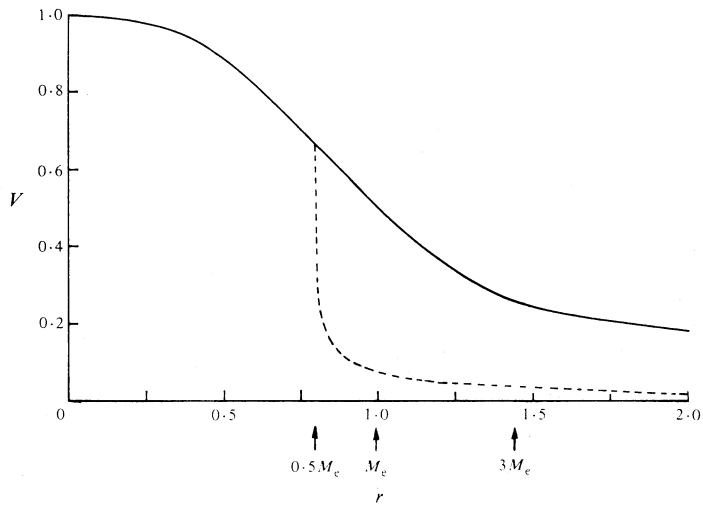

Fig. 5. Approximate representation of the expansion of a supernova shell in a uniform medium (solid curve). The radius r is normalized to unity for $M_s = M_e$. The dashed curve shows the result of impacting on the inner surface of a 'bubble' for which the ratio of densities is 100 : 1.

In Fig. 5 the application of these equations is shown for the simple case of expansion into a uniform medium. The transition between them is mainly effected while M_s changes from M_e to $3M_e$. Some numerical calculations on a particular model have suggested that the self-similar adiabatic regime would not be fully established until $M_s \sim 10M_e$ (Jones *et al.* 1981); a value larger than $3M_e$ for full establishment appears likely as a general rule because our approximations are expected to lead to lower limits.

For a remnant expanding into a uniform medium of normal composition we may therefore conservatively regard the remnant as entering the adiabatic phase at a diameter corresponding to $M_s \geqslant 3M_e$, given by

$$D_a \geqslant 6(M_e/M_\odot n)^{\frac{1}{3}} \text{ pc},$$

where n is the density of the medium in cm^{-3}. Thus for ejecta of mass $4M_\odot$ expanding into a uniform medium for which $n = 0{\cdot}01$ we find $D_a \geqslant 44$ pc. Tycho's supernova is of special interest as it appears to be approaching the adiabatic phase (Strom *et al.* 1982). On assuming an ejecta mass $\sim 1M_\odot$, consistent with its classification as a Type I SNR, the density indicated for the interstellar medium is $n \sim 0{\cdot}2\ \text{cm}^{-3}$.

For a remnant developing in a cavity previously formed either by a stellar wind or an earlier supernova explosion (see Section 7*b*), the velocity may drop very sharply when the inner surface of the cavity is encountered; the dashed curve in Fig. 5 shows the effect of impacting on a cavity surface when the ratio of the interstellar medium densities is 100 : 1 and the mass of the cavity medium is half that of the ejecta.

While these results give an approximate description of the development of SNR shells, they are not directly related to the evolution of the radio emission. There is no generally accepted theory for the development of radio emission in a shell and, in the case of Type II supernovae, it may well be strongly influenced by the injection of relativistic electrons from a neutron star remnant. Even here, however, magnetic fields are needed for synchrotron radiation and some calculations by Gull (1973) have suggested the importance of Rayleigh–Taylor instabilities at the ejecta–medium interface in causing turbulence which amplifies magnetic fields and also accelerates particles. The mechanism of van de Laan (1962) operates on the simple compression of the interstellar magnetic field by the expanding remnant and might also be important. Whatever the actual mechanism, it seems likely that the deceleration of ejecta by interaction with the interstellar medium is important for the development of emission. Thus the development of strong radio emitting shells might be expected when the ejecta interact with a previously blown bubble. This process might account for the strongly emitting remnants of large diameter found in the Clouds. Conversely, the low-luminosity small-diameter remnants might represent shells only slightly decelerating in a low-density environment. It will be interesting to monitor these for luminosity changes.

For small to intermediate diameters the low slope for the *N–D* relation can reasonably be explained as the result of initial expansion of most of the remnants in a medium of low density, but the evolution of decelerated remnants must also be considered. If the radio emission persists after slowing, the *N–D* slope will increase with increasing diameter as a greater proportion of the remnants are slowed. This increase in slope is not observed; in fact the slope decreases for diameters greater than about 40 pc. Incompleteness for large diameter remnants will contribute to a decrease but it is improbable that it can account as well for the lack of increase. There seems to be no easy way to avoid the conclusion that, not long after the onset of strong interaction with the interstellar medium, there is a rapid diminution of synchrotron radio emission. The conventional adiabatic assumption leads to a relation of the form $L \propto D^{-4}$ (Shklovskii 1968), i.e. $L \propto t^{-1{\cdot}6}$. Such a slow rate of decrease cannot account for the marked scarcity of remnants with luminosities between about 3×10^{16} and $\sim 10^{15}\ \text{W Hz}^{-1}$, the approximate sensitivity limit of our equipment. It therefore seems necessary to postulate the disruption and rapid

dissipation of the radio emitting shell not long after it has reached maximum emission so that it no longer stands out clearly above the general background. The possible cause of such behaviour is obscure but the appearance of a number of remnants is suggestive, e.g. 0047–735, 0050–728, 0455–687, 0534–699 and 0543–689. The morphology of some Galactic remnants might also be explicable in this way.

The optical SNRs in the Clouds catalogued by Mathewson *et al.* (1983) have a very similar N–D relation to the one we find; applying the maximum likelihood method to the sizes listed in their paper for diameters $\leqslant 40$ pc, we find that $\beta = 1{\cdot}1 \pm 0{\cdot}2$. The similarity to the radio result is hardly surprising as the recognition of optical remnants was predicated on the observation of X-ray emission; no non-radio SNRs were catalogued. On the basis of the evolution discussed above, however, it seems that there might be significant numbers of optical remnants remaining in which the radio remnant had dissipated. These would be characterized by predominantly thermal radio emission and might be represented by the flat spectrum shells and rings that have no readily identifiable exciting stars. We have included two such possible SNRs in our maps, 0536–692 and 0543–678 (N70). The former has some evidence for associated non-thermal and X-ray emission on the eastern side (Clarke *et al.* 1976; Long *et al.* 1981).

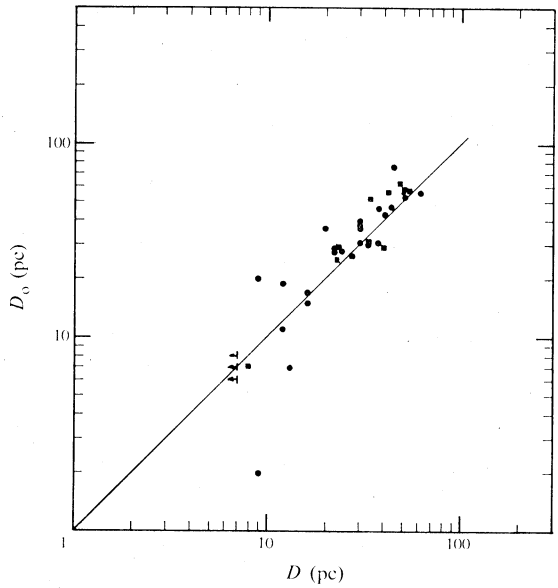

Fig. 6. Comparison of radio diameters D and optical diameters D_o of SNRs in both Magellanic Clouds.

7. SNR Morphology

The remnants in the Magellanic Clouds present a unique opportunity to study the morphology of an essentially complete sample. The larger remnants are here well resolved and their main features clearly delineated. However, the resolution is inadequate to provide a great deal of information about the smaller remnants and these must await studies with the higher resolution of future instruments. Nevertheless it is possible to recognize a clearly distinct class of small diameter remnants.

(*a*) *Centrally Concentrated SNRs*

As shown in Fig. 6, the majority of remnants have radio sizes comparable with that of the optical shell. In most cases the small differences can be ascribed to different

operational definitions. Two examples in which the SNRs 0538–691 and 0540–693 have radio sizes much larger than the optical size might be the result of unassociated background emission as indicated in the footnotes to Table 1. In another example, 0535–660 (LHG59, N63A), the radio remnant is twice and the X-ray remnant three times the optical size (Mathewson *et al.* 1983), an exceptional situation which merits further investigation.

There are also a few cases in the LMC for which the radio size is clearly smaller than the optical size. These include 0453–685 (LHG1), 0505–679 (LHG10) and 0543–689 (LHG82). The three unresolved SNRs, 0509–687 (LHG13, N103B), 0509–675 (LHG14) and 0519–690 (LHG26) could also be in this category. For the large SNR 0543–689 (LHG82) the discrepancy in size is unlikely to be significant; it is of very low surface brightness and badly defined. For the small diameter remnants, however, the positions of the radio centroids agree closely with the optical centres given by Mathewson *et al.* (1983) and the presence of a centrally concentrated component is indicated, possibly associated with a neutron star. These remnants are suggestive of 'filled-centre' types recognized in the Galaxy but, unlike the better known remnants of this type, have an X-ray structure apparently associated with the shell.

The very weak 0505–679 (LHG10) remnant is the most interesting. It is barely resolved but the thermal emission from the optical shell of 1·2 arcmin diameter is estimated to be about 3–4 mJy (using the Hβ flux of Tuohy *et al.* 1982); this is a third or more of the total flux density. The remaining emission must be strongly concentrated towards the centre to give the fitted size of 35 arcsec. The remnant is one of the four shells with Balmer dominated spectra which Tuohy *et al.* (1982) attribute to Type I supernovae. Two others, 0509–675 (LHG14) and 0519–690 (LHG26) are unresolved with indications that the radio size could be substantially less than the optical size, while the fourth, 0548–704 (LHG89) displays markedly bipolar radio structure rather smaller than the optical shell.

In all these cases the radio observations are consistent with the presence of an active neutron star remnant; on current views this is more suggestive of Type II SNRs. Certainly the Galactic Type I SNRs have a different morphology in which the shell emission dominates. The abnormal optical spectra might arise from expansion in a partially ionized medium of exceptionally low density as suggested by Tuohy *et al.* (1982); the weakness of synchrotron emission from the shells would support this interpretation. The SNR 0453–685 (LHG1) appears to have similarities in the radio structure and might perhaps represent a more evolved remnant of the same type. The observed presence of [O III] emission in this shell (Mathewson *et al.* 1983) would not be inconsistent; the line is already detectable in the LHG10 remnant.

Higher resolution is needed for further study of these remnants, but the present resolution is quite adequate to explore the morphology of a substantial group of the larger remnants.

(*b*) *Well-resolved SNRs*

Large diameter remnants are often referred to as 'old' or 'evolved' and the low radial velocities of the optical filaments regarded as clinching evidence. In view of our results, however, these descriptions do not seem appropriate; we find an age of $\sim$3000 yr for a 40 pc diameter remnant and a mean expansion velocity of $\sim$7000 km s^{-1}. One interpretation is that such remnants have been formed comparatively

recently as a result of an expanding shell impacting on the inner surface of a previously formed bubble within which the supernova has exploded. Such a bubble might be formed by the stellar wind of a massive star which eventually became the supernova or by the stellar winds of groups of early type stars near the supernova or even by previous nearby supernovae. One remnant at least appears to support such an interpretation, 0547–697 (N135). It has a dumb-bell shape but our map (see Appendix, map 21) shows that there is no enhancement of emission at the central constriction as would be expected if we were observing the chance overlap of two separate remnants along the line of sight. A more plausible explanation is that two 'old' bubbles have coalesced and a supernova later exploded close to their junction.

At the other extreme, a substantial class of low luminosity remnants shows a closely circular outline. It is difficult to see how these could have arisen as the result of an old evolved remnant. For such a remnant the mean velocity of expansion of any substantial part of the shell is critically dependent on the density of the interstellar medium which it encounters during its expansion. An irregular medium would suggest an irregular outline and one might expect that regions of high interaction would lead to higher radio emission as well as lower mean expansion velocities. Approximately circular large remnants of low luminosity would seem to have suffered little retardation, and the bright optical filaments might be ascribed to prior filamentary condensations in the interstellar medium which the remnant is rapidly sweeping past and only partially accelerating.

The three-dimensional forms of the remnants cannot be known with certainty as we observe only a two-dimensional projection. Nevertheless it is interesting to speculate on the real forms and how they might be produced. Noteworthy is the occurrence of 'bipolar' circular remnants with two nearly equal maxima of emission. These are represented by 0046–735, 0049–736, 0520–694, 0532–710 and 0534–699; they include more than one-quarter of all remnants with diameters greater than 30 pc. Another common form is the 'horseshoe' type, almost circular again but with very low emission over part of the circumference. Examples of this type are 0050–728, 0058–718, 0103–726, 0528–692, 0536–706 and 0538–691; they represent about one-third of the remnants with diameters greater than 30 pc.

In the 'bipolar' remnants, the distribution is quite symmetrical and could be represented by a spherical shell with a belt of strong emission superimposed, observed, of course, in random orientations. A well known explanation for this morphology in Galactic SNRs is that a belt of strong emission is caused by the preferential compression of the Galactic magnetic field due to expansion normal to the field; as an alternative explanation, one might consider the injection of relativistic electrons along the belt by a spinning neutron star. The second 'horseshoe' form almost certainly arises from the absence of part of a radio emitting shell and implies an asymmetric process, possibly in the initial ejection, although alternative possibilities are the prior formation of an elongated cavity by the motion of the wind-producing star or stars, or the occurrence of a supernova near the edge of a cavity. These possibilities are speculative and could only be tested by numerical modelling, taking into account also data available from optical spectra and the distribution of X-ray emission.

8. Conclusions

The SNRs in the Magellanic Clouds display a great diversity of properties which makes statistical analysis rather uncertain. It may be reasonably assumed that the

Galactic SNRs have a similar diversity; intercomparisons have revealed no significant differences between the two populations. Although the *N–D* relations cannot be defined very accurately in either the Clouds or the Galaxy, they appear to be similar in each and to imply that the majority of remnants have expanded rapidly to their present sizes with little deceleration for the greater part of their lifetime. This is consistent with a preferential occurrence of supernovae in low density regions of the interstellar medium, possibly in previously formed bubbles. As a corollary, it appears that the radio remnant must either decay rapidly or be dissipated not long after the expansion has slowed significantly and the remnant entered the 'Sedov' regime. Thus we look on the typical radio SNR as a transient phenomenon with an active lifetime measured in thousands of years rather than tens of thousands. The size of a luminous (well decelerated) remnant is then largely determined by the initial density and distribution of the interstellar medium in the vicinity of the supernova.

Comparison of well determined distances of Galactic remnants with distances derived from a scale based on the Cloud remnants shows good agreement. A small systematic difference between the Cloud calibrated distances and the kinematic distances derived by radio line absorption measurements would be easily resolved if the distance to the Galactic centre were somewhat less than the 10 kpc assumed in the rotational model. Comparison with optically derived distances also yields good agreement but, if these are used as standards, a slight reduction in our assumed distances of the Clouds is suggested (to about 49 and 60 kpc). The indicated accuracy of these measures is about 10%.

We have made no attempt to differentiate between shell and centrally-concentrated types in deriving the statistical properties. Both types can be recognized in the Clouds and some better correlations might be obtained if they were separated. However, we consider that it is necessary to understand the relation between them before making arbitrary divisions.

Note added in proof: The 'possible' SNR, 0536−692, has now been confirmed as the result of optical and X-ray data (Mathewson, Ford, Dopita, Tuohy, Mills, Turtle and Helfand; in preparation).

Acknowledgments

Operation of the Molonglo Observatory Synthesis Telescope is supported by the Australian Research Grants Scheme and by the University of Sydney. The computer programs for the preparation of the published maps have been written by Dr D. F. Crawford.

References

Chevalier, R. A. (1974). *Astrophys. J.* **195**, 53.
Clark, D. H., and Caswell, J. L. (1976). *Mon. Not. R. Astron. Soc.* **174**, 267.
Clark, D. H., and Stephenson, F. R. (1977*a*). 'The Historical Supernovae' (Pergamon: Oxford).
Clark, D. H., and Stephenson, F. R. (1977*b*). *Mon. Not. R. Astron. Soc.* **179**, 87P.
Clarke, J. N. (1976). *Mon Not. R. Astron. Soc.* **174**, 393.
Clarke, J. N., Little, A. G., and Mills, B. Y. (1976). *Aust. J. Phys. Astrophys. Suppl.* No. 40, 1.
Crawford, D. F., Jauncey, D. L., and Murdoch, H. S. (1970). *Astrophys. J.* **162**, 405.
Davies, R. D., Elliott, K. H., and Meaburn, J. (1976). *Mem. R. Astron. Soc.* **81**, 89.
Durdin, J. M., Little, A. G., and Large, M. I. (1984). URSI/IAU. Symp. on Indirect Imaging, August 1983 (Ed. J. A. Roberts), p. 75 (Cambridge Univ. Press).

Goss, W. M., Schwarz, U. J., Ekers, R. D., and van Gorkom, J. H. (1983). IAU Symp. 101 on Supernova Remnants and Their X-Ray Emission (Eds J. Danziger and P. Gorenstein), p. 65 (Reidel: Dordrecht).
Gull, S. F. (1973). *Mon. Not. R. Astron. Soc.* **161**, 47.
Henize, K. G. (1956). *Astrophys. J. Suppl.* **2**, 315.
Inoue, H., Koyama, K., and Tanaka, Y. (1983). IAU Symp. 101 on Supernova Remnants and Their X-Ray Emission (Eds J. Danziger and P. Gorenstein), p. 535 (Reidel: Dordrecht).
Jones, E. M., Smith, B. W., and Straka, W. C. (1981). *Astrophys. J.* **249**, 185.
Long, K. S. (1983). IAU Symp. 101 on Supernova Remnants and Their X-Ray Emission (Eds J. Danziger and P. Gorenstein), p. 525 (Reidel: Dordrecht).
Long, K. S., Helfand, D. J., and Grebalsky, D. A. (1981). *Astrophys. J.* **248**, 925.
McGee, R. X., Brooks, J. W., and Batchelor, R. A. (1972). *Aust. J. Phys.* **25**, 581.
McKee, C. F., and Ostriker, J. P. (1977). *Astrophys. J.* **218**, 148.
Mathewson, D. S., Ford, V. L., Dopita, M. A., Tuohy, I. R., Long, K. S., and Helfand, D. J. (1983). *Astrophys. J. Suppl.* **51**, 345.
Mathewson, D. S., Ford, V. L., Dopita, M. A., Tuohy, I. R., Mills, B. Y., and Turtle, A. J. (1984). Supernova remnants in the Magellanic Clouds. *Astrophys. J.* (in press).
Mills, B. Y. (1981). *Proc. Astron. Soc. Aust.* **4**, 156.
Mills, B. Y. (1983). IAU Symp. 101 on Supernova Remnants and Their X-Ray Emission (Eds J. Danziger and P. Gorenstein), p. 551 (Reidel: Dordrecht).
Mills, B. Y., Little, A. G., Durdin, J. M., and Kesteven, M. J. L. (1982). *Mon. Not. R. Astron. Soc.* **200**, 1007.
Mills, B. Y., and Turtle, A. J. (1984). IAU Symp. 108 on Structure and Evolution of the Magellanic Clouds (Eds S. van den Berg and K. de Boer), p. 283 (Reidel: Dordrecht).
Mills, B. Y., Turtle, A. J., and Watkinson, A. (1978). *Mon. Not. R. Astron. Soc.* **185**, 263.
Milne, D. K., Caswell, J. L., and Haynes, R. F. (1980). *Mon Not. R. Astron. Soc.* **191**, 469.
Seward, F. D., and Mitchell, M. (1981). *Astrophys. J.* **243**, 736.
Shklovskii, I. S. (1968). 'Supernovae' (Wiley: London).
Srinivasan, G., and Divarakanath, K. S. (1982). *Astron. Astrophys.* **3**, 351.
Strom, R. G., Goss, W. M., and Shaver, P. A. (1982). *Mon. Not. R. Astron. Soc.* **200**, 473.
Tammann, G. A. (1977). *Ann. N. Y. Acad. Sci.* **302**, 61.
Tuohy, I. R., Dopita, M. A., Mathewson, D. S., Long, K. S., and Helfand, D. J. (1982). *Astrophys. J.* **261**, 473.
van der Laan, H. (1962). *Mon. Not. R. Astron. Soc.* **124**, 125.

Appendix

Maps of 24 SNRs and possible remnants in the Large Magellanic Cloud are presented on pp. 345–57. The map parameters are given in Table 5. Generally, the maps are 'uncleaned' and the beam has a first negative sidelobe of -8%; other sidelobes are less than 1%. However, maps 4, 18 and 19 have been 'cleaned' to remove the effects of the negative sidelobe and reveal the structure more clearly. The beamwidth is 43×43 cosec δ arcsec and is shown on each map at the relative position indicated in the fifth column of Table 5. Coordinate grid marks are at 10^s in right ascension and $1'$ in declination.

Manuscript received 19 December 1983, accepted 6 March 1984

Table 5. Parameters of the maps of 24 supernova remnants

Map	Radio source	LHG[B]	N[C]	FWHM beam[D]	Peak (mJy/beam)	Contour levels (percentage of peak)															
1	0453–685	1		TR	83·3	90		70		50	40		30		20	15		10	±6	±3		
2	0454–665		11L	BR	73·9	90		70		50	40		30		20	15		10	±6	±3		
3	0455–687	2	86	BR	45·9	90		70		50	40		30		20		±12		±6			
4[A]	0500–702	7	186D	TR	15·5	90		70		50	40		30		20			±10				
5	0505–679	10		BL	8·5		80		60		40				±20							
6	0506–680	11	23	TR	215	90		70		50			30		20			10	7	±5	±3	±1·5
7	0519–697	23	120	TL	548	90		70		50			30		20	15	12·5	10	7·5	5	±3	±2
8	0520–694	27		BL	20·4	90	80	70	60	50	40		30		±20			±10				
9	0525–660	34		TL	150	90	80	70	60	50	40		30		20			10	±6	±4	±2	
10	0525–696	35	132D	BL	2124	90		70		50	40		30		20			10		±5	±2	
11	0525–661	36	49	BL	905	90		70		50			30		20			10		±5	±2	
12	0527–658	39		TR	14·1	90		70		50	40		30		±20	±15		±10				
13	0532–710	47	206	TL	53·9	90	80	70	60	50	40		30		20			±10	±4			
14	0534–699	53		BL	40·5	90		70		50	40	35	30	25	20	15		±10	±5			
15	0534–705	54		BR	15·4	90	80	70	60	50	40		30		20			±10				
16	0535–660	59	63A	BR	1410	90		70		50			30		20			10	±5	±3	±1	
17	0536–706	61		TR	12·0	90	80	70	60	50	40		30		±20							
18[A]	0538–691	67	157B	BR	864	90	80	70	60	50	40		30		20			10	6	4	±2	±1
19[A]	0540–693	79		BR	582	90	80	70	60	50	40		30		20			10	5	3	±1·5	
20	0543–689	82		TR	12·9	90		70		50			30		±20			±10				
21	0547–697	88	135	BR	77·7	90	80	70	60	50	40		30		20	15		±10	±4			
22	0548–704	89		BL	23·2	90	80	70	60	50	40		30		20			10				
23	0536–692			TR	179	90	80	70	60	50	40		30		20	15		10	±6	±3		
24	0543–678		70	BR	8·7	90		70		50		35			±20							

[A] Map has been cleaned.
[B] Long, Helfand and Grabelsky (1981).
[C] Henize (1956).
[D] FWHM beam is the ellipse in the designated corner of each map (Top, Bottom, Left, Right).

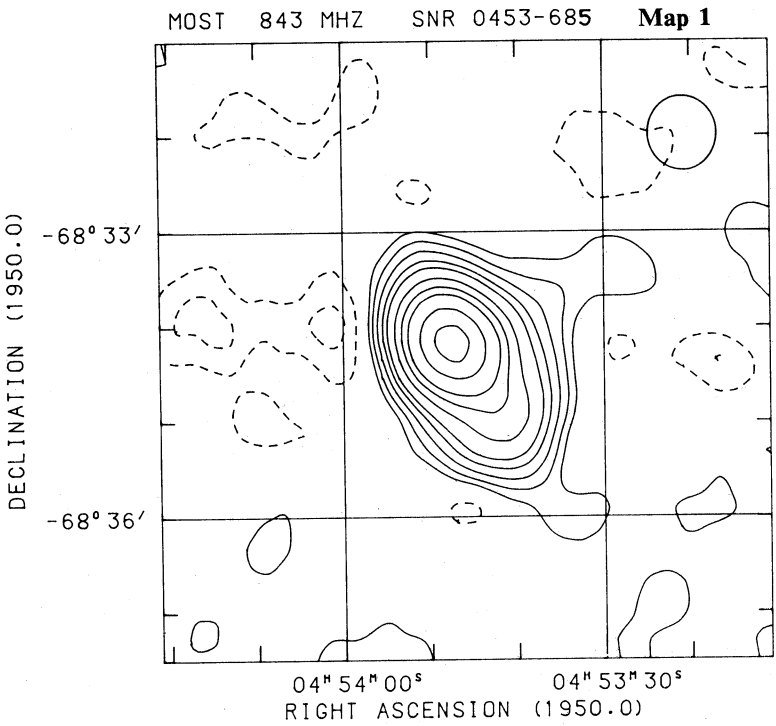
MOST 843 MHZ SNR 0453-685 Map 1
DECLINATION (1950.0)
-68° 33′
-68° 36′
04ᴴ 54ᴹ 00ˢ
04ᴴ 53ᴹ 30ˢ
RIGHT ASCENSION (1950.0)

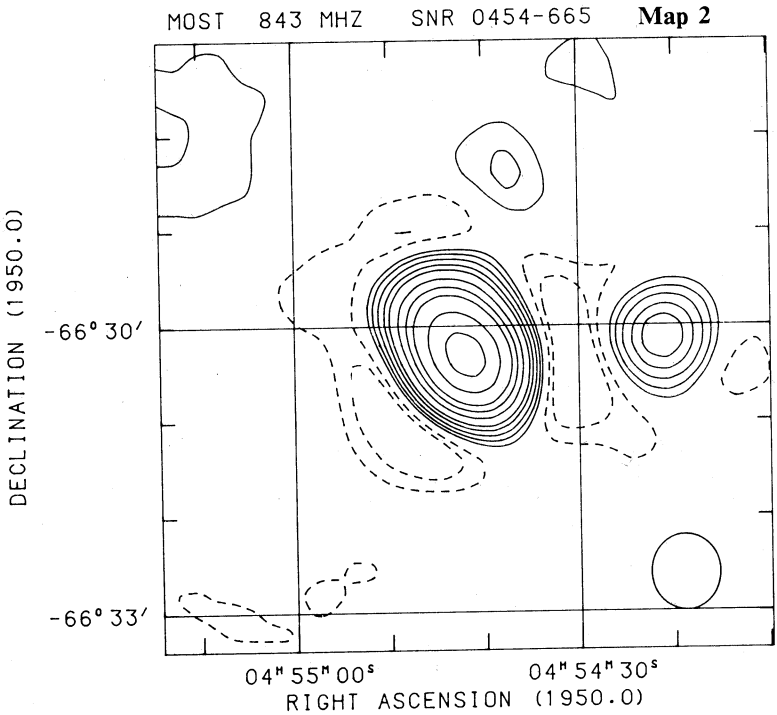
MOST 843 MHZ SNR 0454-665 Map 2
DECLINATION (1950.0)
-66° 30′
-66° 33′
04ᴴ 55ᴹ 00ˢ
04ᴴ 54ᴹ 30ˢ
RIGHT ASCENSION (1950.0)

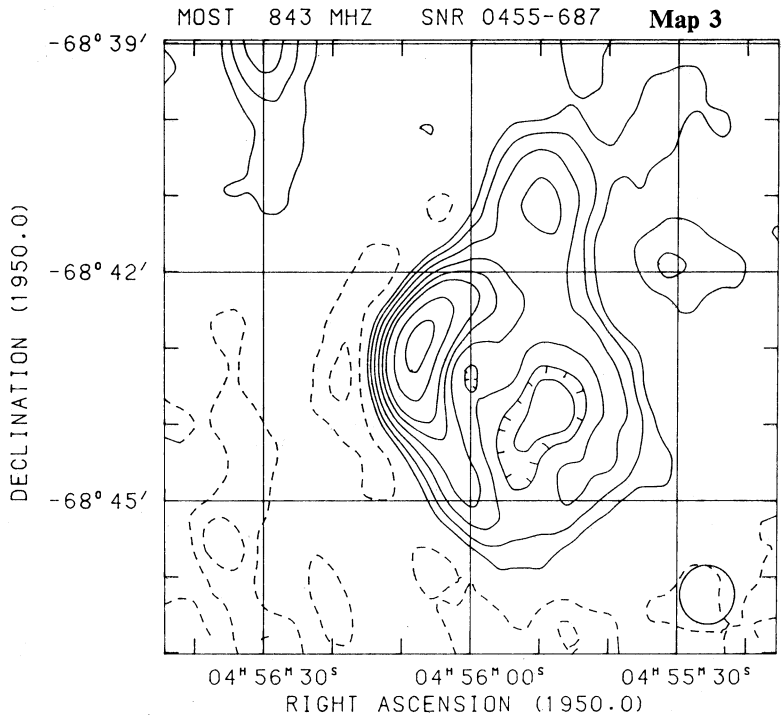
MOST 843 MHZ SNR 0455-687
Map 3
-68° 39′
-68° 42′
-68° 45′
DECLINATION (1950.0)
04ᴴ 56ᴹ 30ˢ
04ᴴ 56ᴹ 00ˢ
04ᴴ 55ᴹ 30ˢ
RIGHT ASCENSION (1950.0)

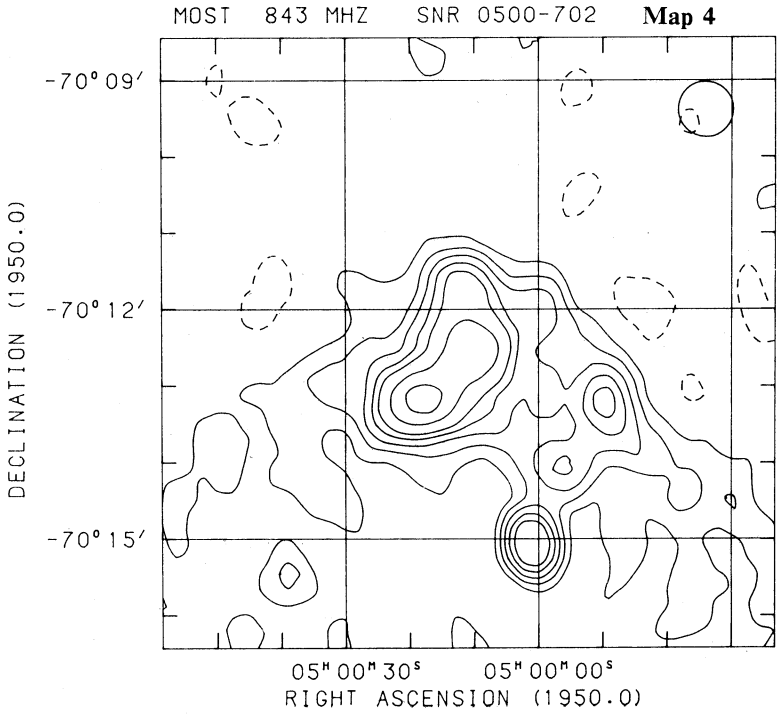
MOST 843 MHZ SNR 0500-702
Map 4
-70° 09′
-70° 12′
-70° 15′
DECLINATION (1950.0)
05ᴴ 00ᴹ 30ˢ
05ᴴ 00ᴹ 00ˢ
RIGHT ASCENSION (1950.0)

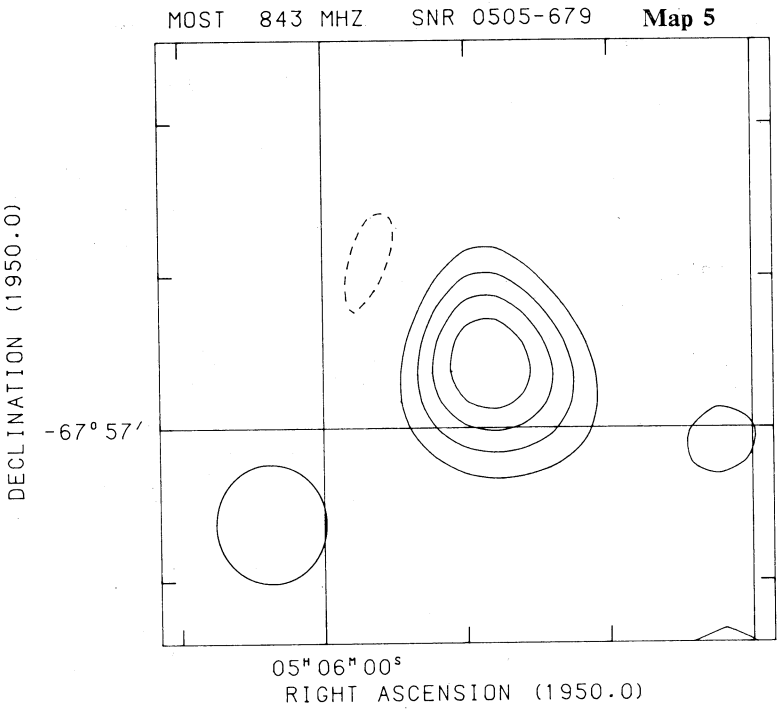
MOST 843 MHZ SNR 0505-679 Map 5
DECLINATION (1950.0)
-67° 57′
05ᴴ 06ᴹ 00ˢ
RIGHT ASCENSION (1950.0)

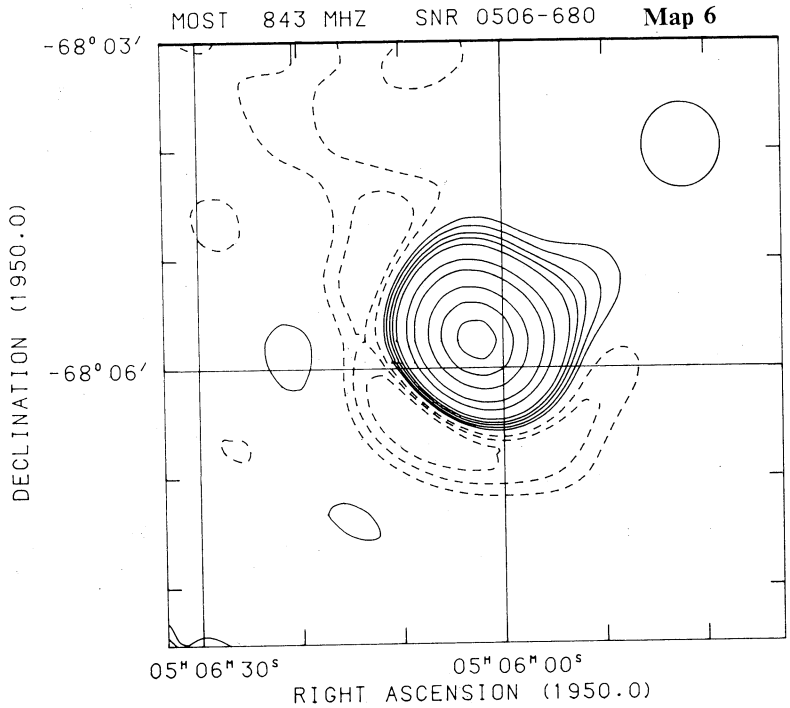
MOST 843 MHZ SNR 0506-680 Map 6
-68° 03′
-68° 06′
DECLINATION (1950.0)
05ᴴ 06ᴹ 30ˢ
05ᴴ 06ᴹ 00ˢ
RIGHT ASCENSION (1950.0)

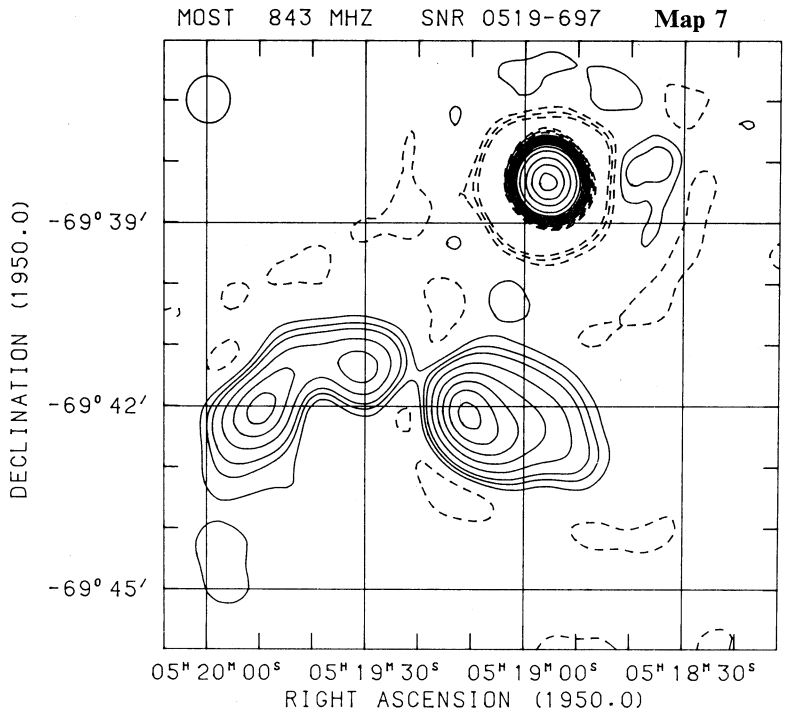
MOST 843 MHZ SNR 0519-697 Map 7
DECLINATION (1950.0)
-69° 39′
-69° 42′
-69° 45′
05ᴴ 20ᴹ 00ˢ 05ᴴ 19ᴹ 30ˢ 05ᴴ 19ᴹ 00ˢ 05ᴴ 18ᴹ 30ˢ
RIGHT ASCENSION (1950.0)

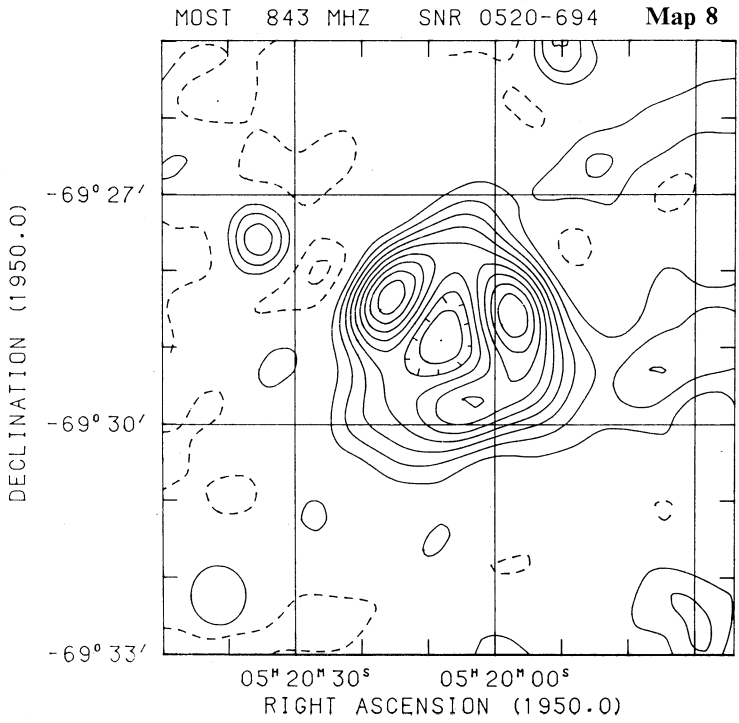
MOST 843 MHZ SNR 0520-694 Map 8
DECLINATION (1950.0)
-69° 27′
-69° 30′
-69° 33′
05ᴴ 20ᴹ 30ˢ 05ᴴ 20ᴹ 00ˢ
RIGHT ASCENSION (1950.0)

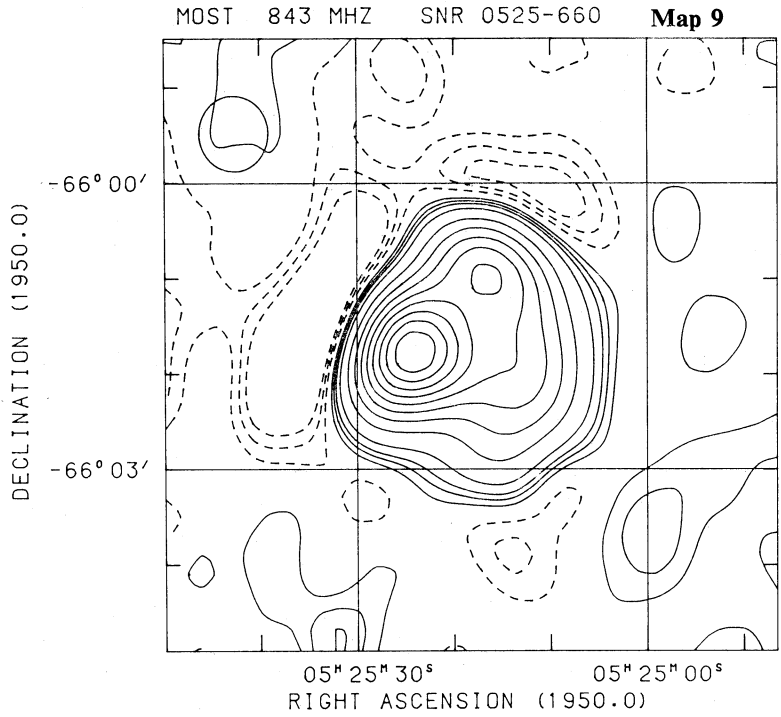
MOST 843 MHZ SNR 0525-660
Map 9
-66° 00′
-66° 03′
DECLINATION (1950.0)
05ᴴ 25ᴹ 30ˢ
05ᴴ 25ᴹ 00ˢ
RIGHT ASCENSION (1950.0)

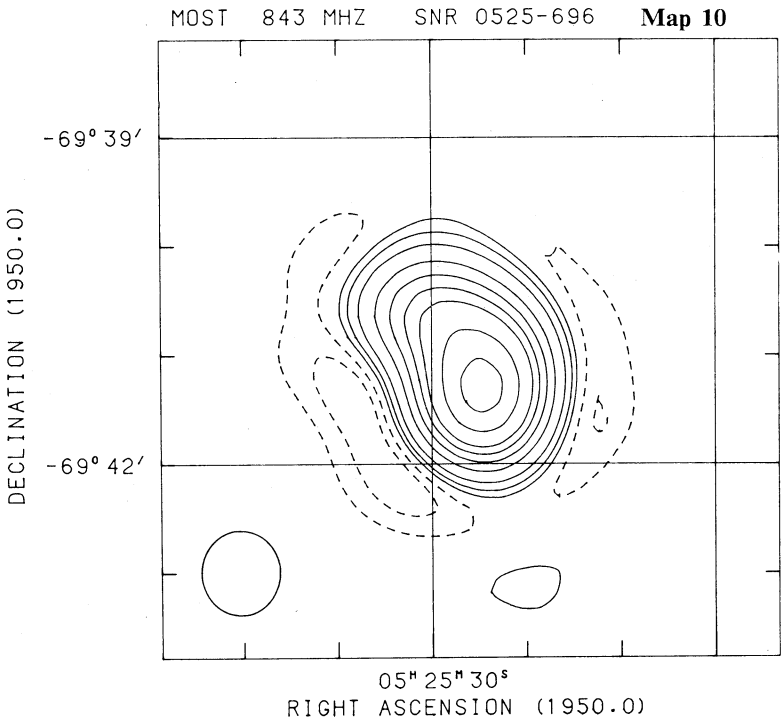
MOST 843 MHZ SNR 0525-696
Map 10
-69° 39′
-69° 42′
DECLINATION (1950.0)
05ᴴ 25ᴹ 30ˢ
RIGHT ASCENSION (1950.0)

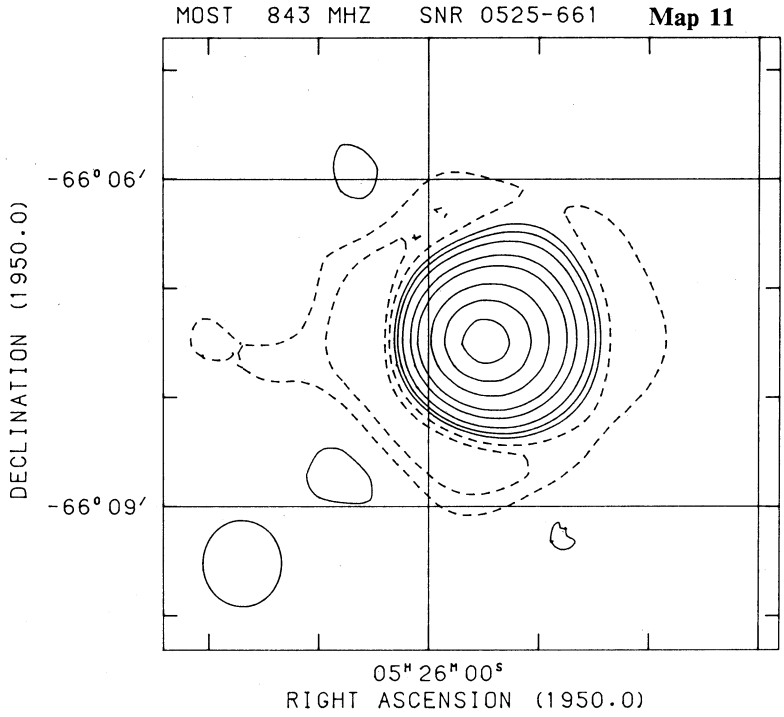
MOST 843 MHZ SNR 0525-661 Map 11
-66° 06′
-66° 09′
DECLINATION (1950.0)
05ᴴ 26ᴹ 00ˢ
RIGHT ASCENSION (1950.0)

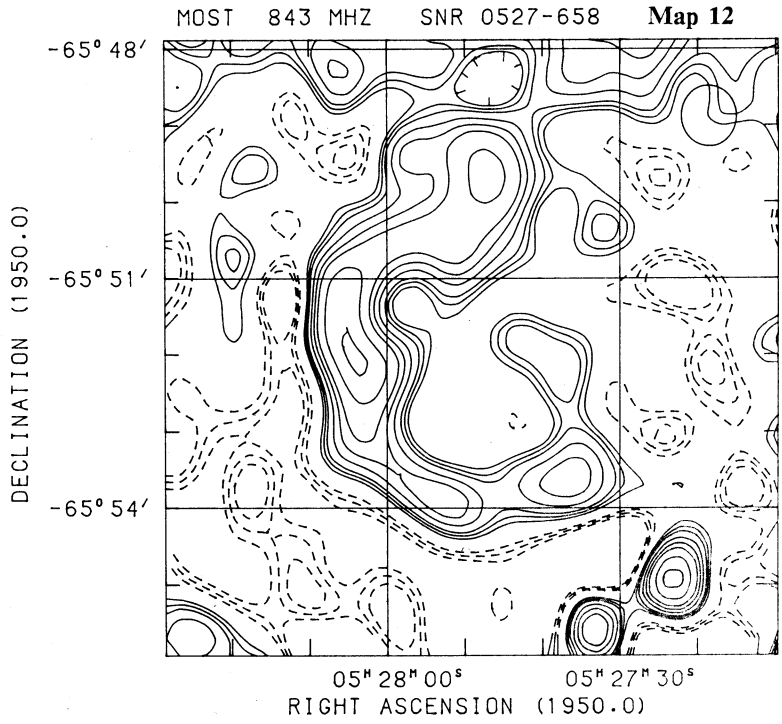
MOST 843 MHZ SNR 0527-658 Map 12
-65° 48′
-65° 51′
-65° 54′
DECLINATION (1950.0)
05ᴴ 28ᴹ 00ˢ
05ᴴ 27ᴹ 30ˢ
RIGHT ASCENSION (1950.0)

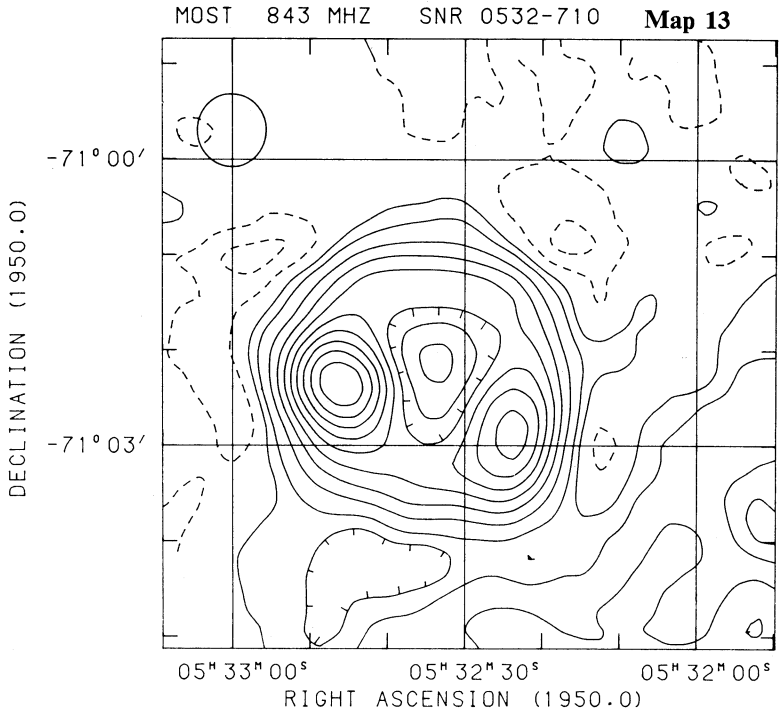
MOST 843 MHZ SNR 0532-710
Map 13
-71°00′
-71°03′
DECLINATION (1950.0)
05ᴴ33ᴹ00ˢ
05ᴴ32ᴹ30ˢ
05ᴴ32ᴹ00ˢ
RIGHT ASCENSION (1950.0)

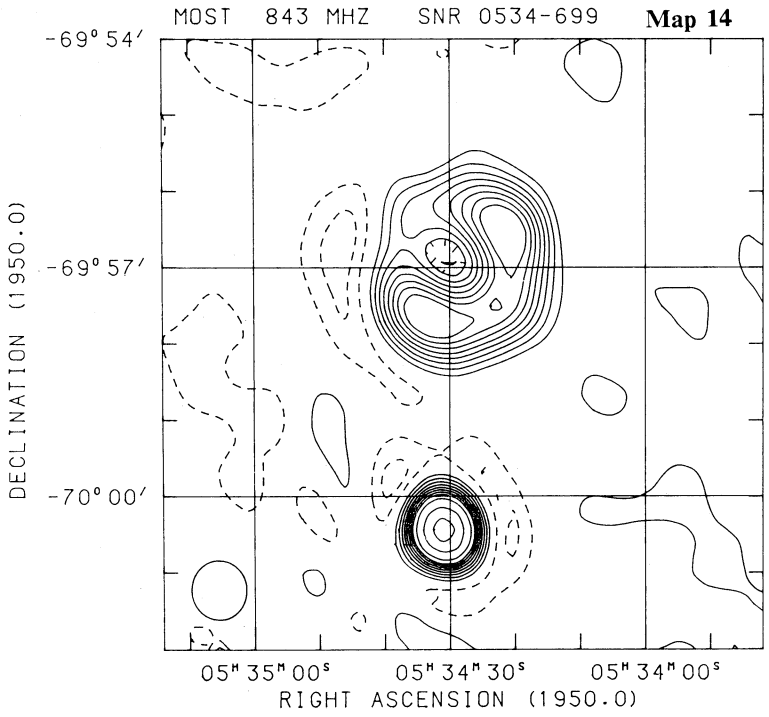
MOST 843 MHZ SNR 0534-699
Map 14
-69°54′
-69°57′
-70°00′
DECLINATION (1950.0)
05ᴴ35ᴹ00ˢ
05ᴴ34ᴹ30ˢ
05ᴴ34ᴹ00ˢ
RIGHT ASCENSION (1950.0)

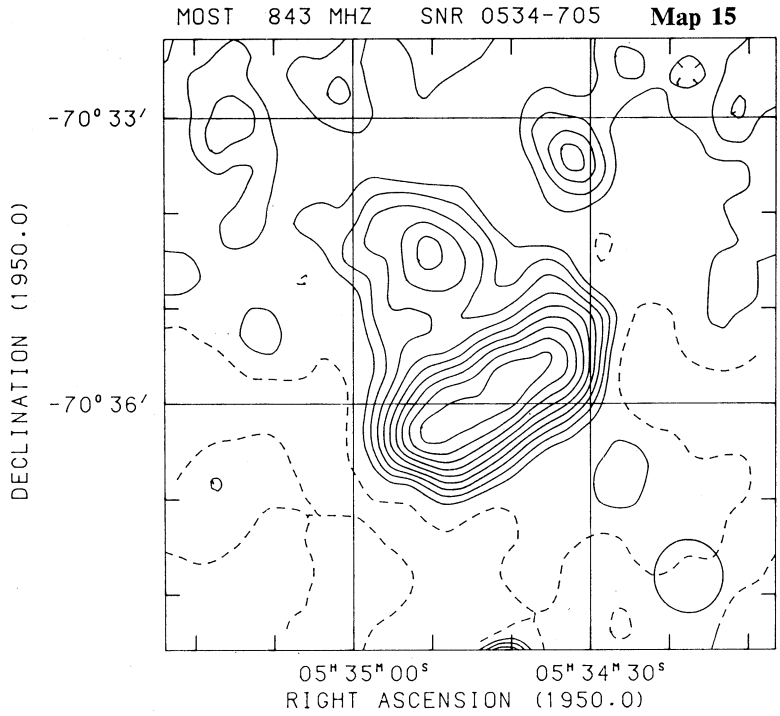
MOST 843 MHZ SNR 0534-705 Map 15
-70° 33′
-70° 36′
DECLINATION (1950.0)
05ᴴ 35ᴹ 00ˢ
05ᴴ 34ᴹ 30ˢ
RIGHT ASCENSION (1950.0)

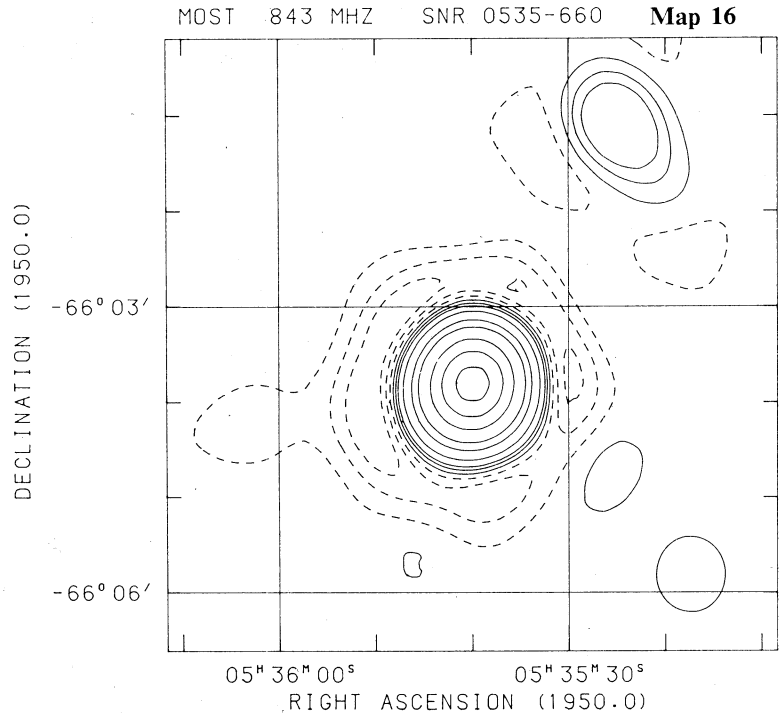
MOST 843 MHZ SNR 0535-660 Map 16
-66° 03′
-66° 06′
DECLINATION (1950.0)
05ᴴ 36ᴹ 00ˢ
05ᴴ 35ᴹ 30ˢ
RIGHT ASCENSION (1950.0)

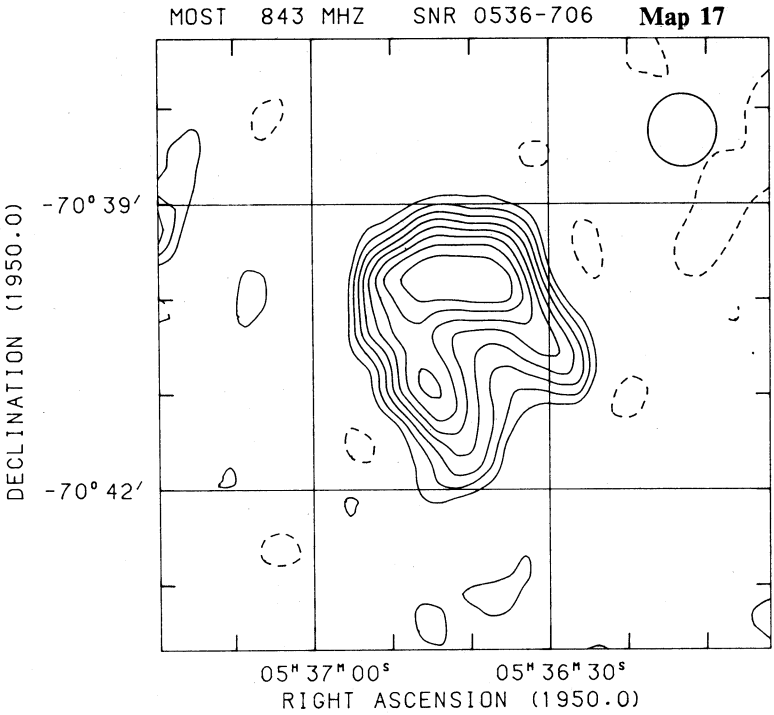
MOST 843 MHZ SNR 0536-706 Map 17
-70° 39′
-70° 42′
DECLINATION (1950.0)
05ᴴ 37ᴹ 00ˢ
05ᴴ 36ᴹ 30ˢ
RIGHT ASCENSION (1950.0)

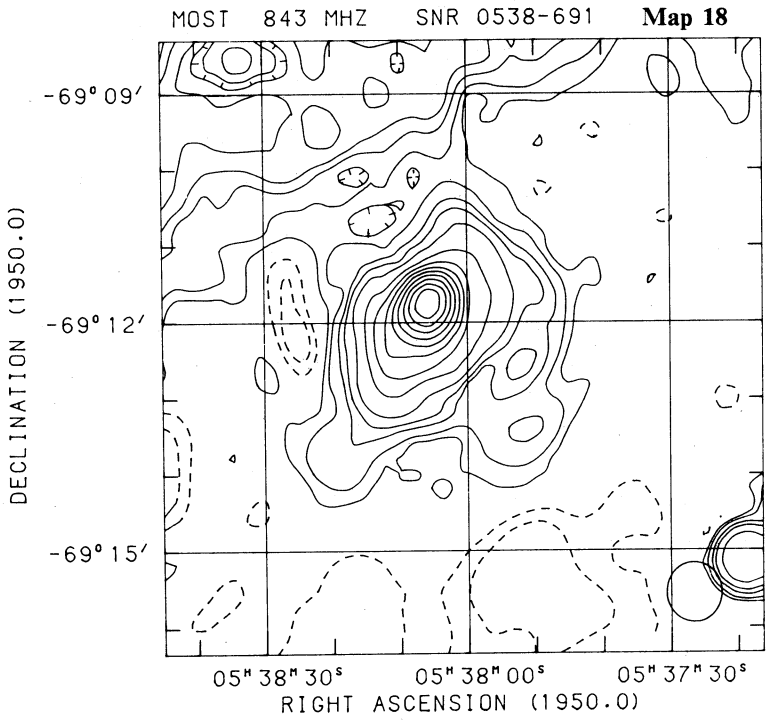
MOST 843 MHZ SNR 0538-691 Map 18
-69° 09′
-69° 12′
-69° 15′
DECLINATION (1950.0)
05ᴴ 38ᴹ 30ˢ
05ᴴ 38ᴹ 00ˢ
05ᴴ 37ᴹ 30ˢ
RIGHT ASCENSION (1950.0)

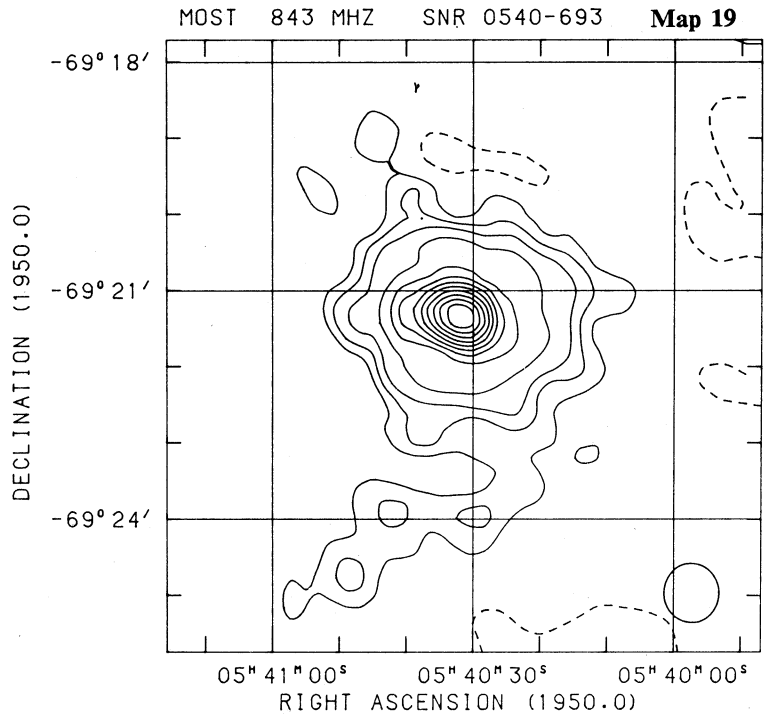
MOST 843 MHZ SNR 0540-693 Map 19
-69° 18′
-69° 21′
-69° 24′
DECLINATION (1950.0)
05H 41M 00S
05H 40M 30S
05H 40M 00S
RIGHT ASCENSION (1950.0)

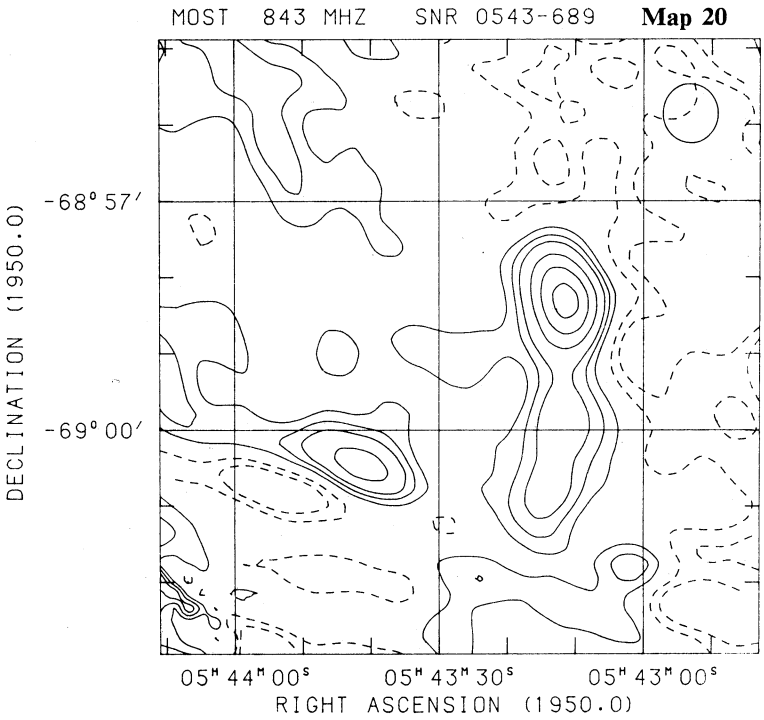
MOST 843 MHZ SNR 0543-689 Map 20
-68° 57′
-69° 00′
DECLINATION (1950.0)
05H 44M 00S
05H 43M 30S
05H 43M 00S
RIGHT ASCENSION (1950.0)

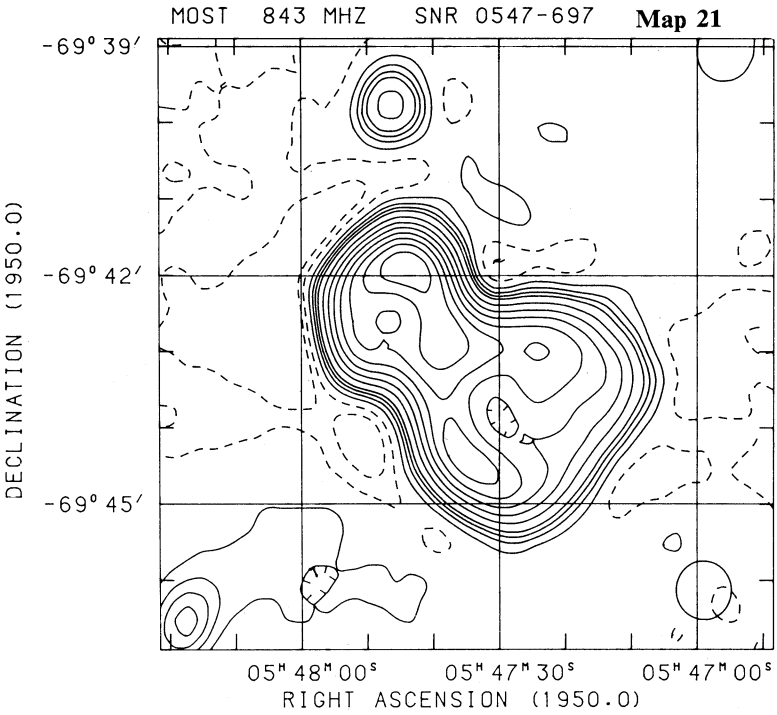
MOST 843 MHZ SNR 0547-697
Map 21
-69° 39′
-69° 42′
-69° 45′
DECLINATION (1950.0)
05ᴴ 48ᴹ 00ˢ
05ᴴ 47ᴹ 30ˢ
05ᴴ 47ᴹ 00ˢ
RIGHT ASCENSION (1950.0)

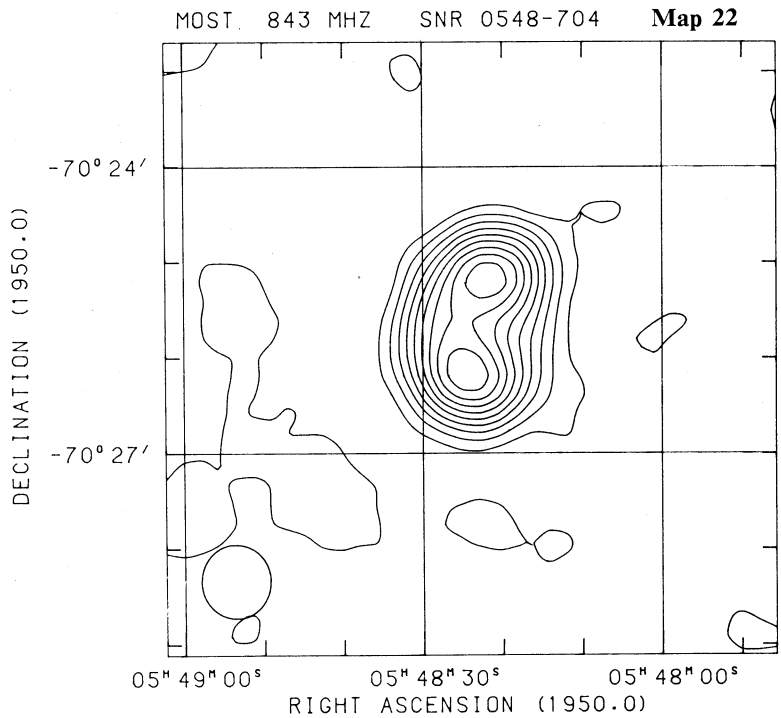
MOST 843 MHZ SNR 0548-704
Map 22
-70° 24′
-70° 27′
DECLINATION (1950.0)
05ᴴ 49ᴹ 00ˢ
05ᴴ 48ᴹ 30ˢ
05ᴴ 48ᴹ 00ˢ
RIGHT ASCENSION (1950.0)

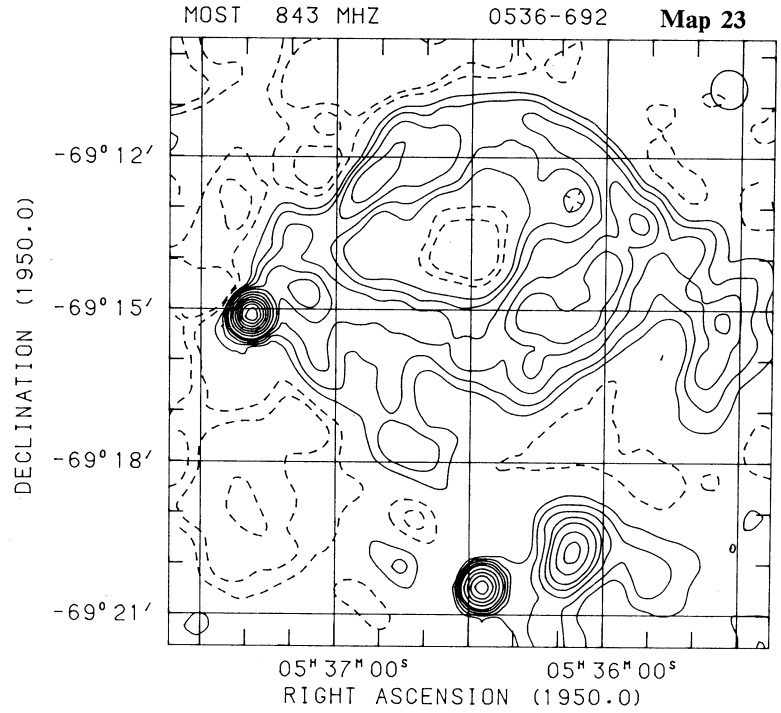
MOST 843 MHZ 0536-692
Map 23
-69° 12′
-69° 15′
-69° 18′
-69° 21′
DECLINATION (1950.0)
05H 37M 00S
05H 36M 00S
RIGHT ASCENSION (1950.0)

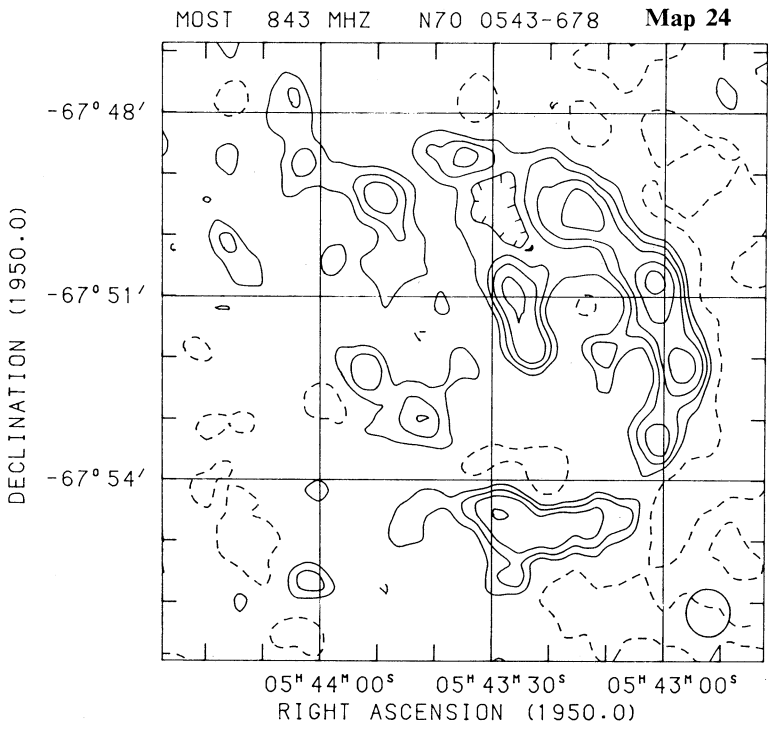
MOST 843 MHZ N70 0543-678
Map 24
-67° 48′
-67° 51′
-67° 54′
DECLINATION (1950.0)
05H 44M 00S
05H 43M 30S
05H 43M 00S
RIGHT ASCENSION (1950.0)